Eldholm, O., Thiede, J., Taylor, E., et al., 1989
Proceedings of the Ocean Drilling Program, Scientific Results, Vol. 104

3. PALEOENVIRONMENTAL SIGNIFICANCE OF CENOZOIC CLAY DEPOSITS FROM THE NORWEGIAN SEA: ODP LEG 104[1]

C. Froget,[2] A. Desprairies,[3] C. Latouche,[4] and N. Maillet[4]

ABSTRACT

The mineralogical and geochemical study of samples from Sites 642, 643, and 644 enabled us to reconstruct several aspects of the Cenozoic paleoenvironmental evolution (namely volcanism, climate, hydrology) south of the Norwegian Sea and correlate it with evolution trends in the northeast Atlantic. Weathering products of early Paleogene volcanic material at Rockall Plateau, over the Faeroe–Iceland Ridge and the Vøring Plateau indicate a hot and moist climate (lateritic environment) existed then. From Eocene to Oligocene, mineralogical assemblages of terrigenous sediments suggest the existence of a warm but somewhat less moist climate at that time than during the early Paleogene. At the beginning of early Miocene, climatic conditions were warm and damp. The large amounts of amorphous silica in Miocene sediment could indicate an important flux of silica from the continent then, or suggest the formation of upwelling. Uppermost lower Miocene and middle to upper Miocene clay assemblages suggest progressive cooling of the climate from warm to temperate at that time. At the end of early Miocene, hydrological exchanges between the North Atlantic and the Norwegian Sea became intense and gave rise to an important change in the mineralogy of deposits. From Pliocene to Pleistocene, the variable mineralogy of deposits reflects alternating glacial/interglacial climatic episodes, a phenomenon observed throughout the North Atlantic.

INTRODUCTION

During ODP Leg 104, eight sedimentary sections ranging from Eocene to Quaternary were drilled at three sites: Site 642 on the outer Vøring Plateau, Site 643 near the lowermost part of the Vøring Plateau, and Site 644 in the inner Vøring Basin (Eldholm, Thiede, Taylor, et al., 1987, and Fig. 1). The aim of this study is to reconstruct paleoenvironmental conditions in the Norwegian Sea using data from bulk mineralogy, mineralogy, and geochemistry of the clay fraction. These analyses may provide information about the source of detrital minerals, the type of climate prevailing at the time of the formation, and determine the oceanic currents responsible for their transport and settling. This type of investigation has already been applied to a large number of Atlantic DSDP sites (Meliéres 1977; Chamley and Robert 1979; Chamley 1979; Chamley et al., 1979; Latouche and Maillet 1979, 1984; Froget 1981; Robert 1982; and Chennaux et al., 1984). Results presented here are compared with those obtained from neighboring drilled sites (DSDP Legs 38, 48B, and 81). Stratigraphic ages referred to in this chapter are from Elliott, Thiede, Taylor, et al. (1987).

METHODS

X-ray Analysis

X-ray diffraction was conducted on 226 samples (CuKα radiation). For Sites 643, 642, and Hole 644B, one sample per core and for each major lithologic change were collected, and for Hole 644A three samples per core.

Total Sediment

Total sediments were analyzed according to the powder diffractogram method: sediments were dried, crushed, and after being set in powder on a support, X-rayed (Brown, 1961). To determine the non-clay minerals involved, we used their characteristic peaks (Joint Committee on Powder Diffraction Standards, 1974): quartz at 3.35 Å, feldspar between 3.23 and 3.16 Å, calcite at 3.035 Å. The peak height characterizing each mineral was applied on a calibration curve, and mineral concentrations were evaluated. Calibration was based on four synthetic reference standards, formed of variable weight mixtures of quartz, feldspars, calcite, and dolomite. Amorphous materials and clay fraction are assumed to form the remainder. Heavy minerals, occurring always in small quantities, were not taken into consideration.

Clay Fraction (<2 μm)

Total sediments were dispersed in deionized water, using mechanical agitation. Samples with calcium carbonate were first treated with N/10 HCl. After several (2 to 3) washings in deionized water and centrifugations, subfractions <2μm were separated by gravity settling. We used the oriented specimen (Brindley and Brown, 1980) method; three slides were prepared for each sample: slide one was scanned untreated, slide two was saturated with ethylene glycol, slide three was heated at 550°C for an hour.

Minerals were identified and examined on the basis of their typical reactions to classical treatment (Brown, 1961; Thorez 1975; Holzapffel, 1985). Peak heights were used to quantify smectite (17 Å), illite (10 Å), and kaolinite plus chlorite (7.1 Å). Chlorite was distinguished from kaolinite on the basis of the difference between their reflections: 002 for kaolinite (3.57 Å) and 004 for chlorite (3.55 Å). Swelling mixed-layer minerals were observed between 10 and 17 Å. Results are given in percentages, evaluated only with regard to the clay minerals in the fraction <2μm. In this fraction, several associated non-clay minerals such as quartz, feldspars, amphiboles, opal CT (Jones and Segnit, 1971) and amorphous silica (displaying a pattern with very broad bands) were observed. Quartz, within the fine-grained fraction, was identified at 4.24 Å (the 3.35-Å peak was superimposed on the illite 003 peak). The abundances of non-clay minerals were estimated in the X-ray diagrams as follows: rare: peak weak; common: peak medium or strong.

Fifty-one powder diagrams were conducted on the <2 μm fractions to obtain, by measurment of d (060), the b parameter of smectites, an estimate of chemical composition (Desprairies, 1983). Values of 060 reflection at 1.51 Å lying at the boundary between dioctahedral and trioctahedral smectites (d-spacing in the range of 1.490–1.500 Å) suggest the presence of aluminous smectites at 1.51 Å, that of ferriferous smectites in the range of 1.52 Å, and that of magnesian smectites at 1.53 Å.

Transmission Electron Microscope (TEM) Observations

TEM was used to examine a highly diluted suspension from the fraction <2μm (Gard, 1971) previously analyzed by X-ray diffraction, to determine the morphology of the clay minerals and detect eventual dia-

---

[1] Eldholm, O., Thiede, J., Taylor, E., et al., 1989. *Proc. ODP, Sci. Results*, 104: College Station, TX (Ocean Drilling Program).

[2] Faculté des Sciences de Luminy, Marseilles, France.

[3] Université de Paris Sud, Orsay, France.

[4] UA197, Université de Bordeaux I, Talence, France.

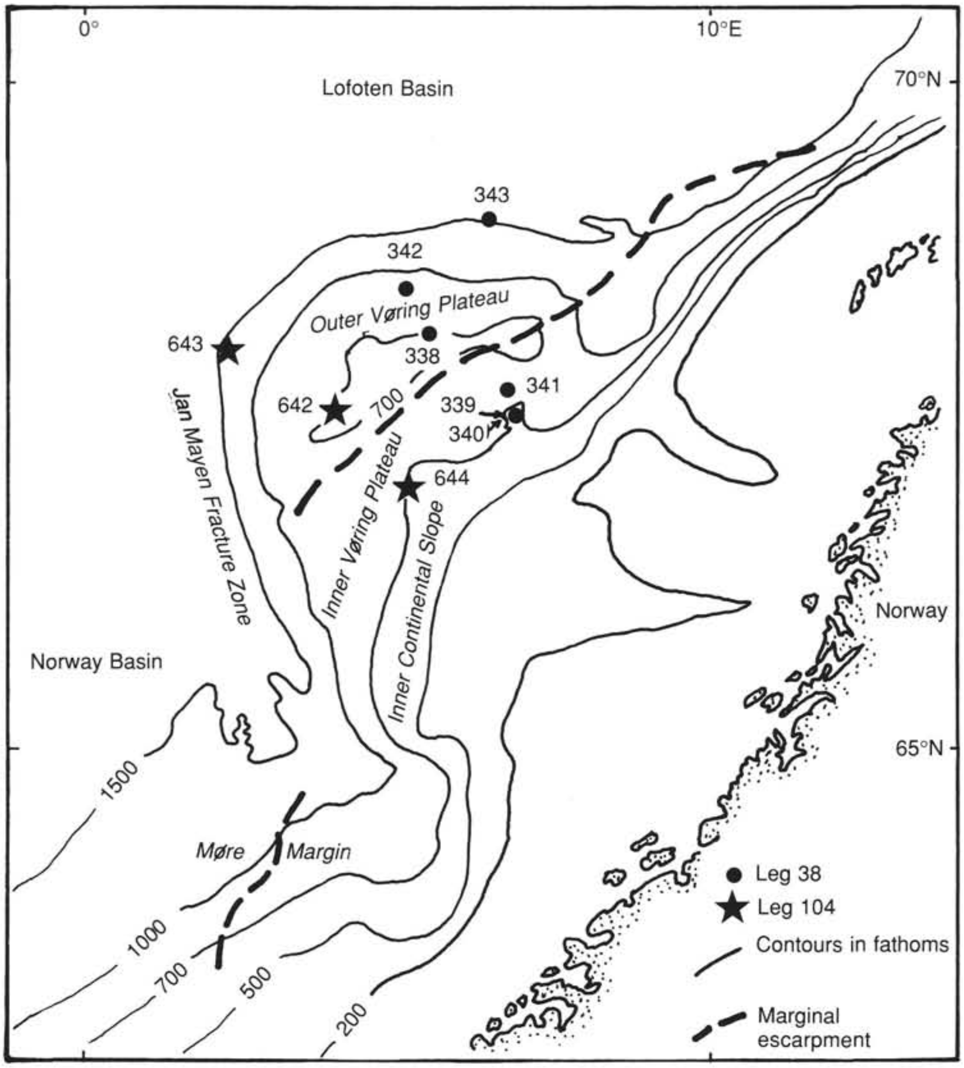

Figure 1. Locations of ODP Leg 104 and DSDP Leg 38 sites drilled in the Norwegian Sea.

genetic phenomena such as lath development around crystals. Fifty levels from Site 643 and six basal levels from Site 642 were examined in this way.

Scanning Electron Microscope (SEM) Analysis

A microscope fitted with an energy-dispersive spectrometer (Si-Li detector, spot size 100 Å, counting time 120 s) was used for analysis of single clay particles (for instance, Fe-Mg illite, see Table 1). Analyses of the clay fraction on crushed and pressed powder were conducted with a SEM fitted with an EDS Linck System (Si-Li detector, scanning area of about 10 mm^2, counting time of 100 s).

RESULTS

Mineralogical Data

We first describe Hole 643A, for it exhibits more complete stratigraphy than Sites 642 and 644. Site to site correlations between lithologic and mineralogical units are given in Figure 2.

Site 643—Hole 643A

Mineralogical assemblages served to distinguish four mineralogical units at Hole 643A (Table 2, Fig. 3).

Mineralogical Unit 1

— Samples 104-643A-62X-1, 79–80 cm to -643A-60X-2, 105–107 cm
— 564.49 to 557.45 mbsf
— Pyroclastic mudstone and basalt rock
— Lower part of lithologic Unit 5
— Non-dated

In bulk sediment samples, the dominant non-clay minerals are quartz and plagioclase feldspars. Smectite (well crystallized) is the preponderant clay mineral (50 to 100%). The 060 reflections indicate a mixture of dioctahedral smectite (1.50 Å), of ferriferous beidellite type, and trioctahedral smectite (1.527 Å) of ferriferous saponite type. In Sample 104-643A-60X-2, 105–107 cm smectites coexist with a mineral at 10 Å and with chlorite. Electron microscopy of samples with the 10-Å reflection revealed the existence of well-shaped individual laths resembling celadonite facies (Plate 1-1); however, the presence of a 002 reflection (5 Å) as well as the chemical composition (Sample 104-643A-61X-1, 19–21 cm; Table 1, analysis 10), imply that samples can best be represented by ferriferous illite rather than glauconite or celadonite species (Weaver and Pollard, 1973).

Mineralogical Unit 2

— Samples 104-643A-57X-4, 68–70 cm to -643A-45X-3, 88–90 cm
— 540.78 to 423.58 mbsf
— Terrigenous mudstone with extremely compact laminations

Table 1. Analyses, water-free basis, structural formula d (060), for smectites (1 to 8), glauconite (9) and Fe-Mg illite (10 and 11) from Leg 38 and Leg 104 sediments. All Fe as Fe_2O_3, oxide values in % weight.

Analysis no.	1	2	3	4	5	6	7	8	9	10	10	10	10	11
Leg	104	38	38	104	104	104	38	38	104			104		104
Hole	643A	343	338	642D	642D	643A	338	338	642A			643A		642D
Core	61-1	12-3	30-4	12-3	13-2	47-2	26-2	24-5	8-1			61-1		8-1
Interval (cm)	80–82	33–35	59–60	31–33	54–56	66–68	42–44	58–60	119–120			19–20		119–230
SiO_2	57.47	60.51	62.05	64.99	65.20	65.5	64.86	64.94	55.18	60.8	61	56.01	56.16	53.64
Al_2O_3	9.33	12.73	12.79	19.47	19.47	18.24	16.74	18.17	5.4	14.45	12.46	21.40	20.29	15.19
Fe_2O_3	15.00	15.17	14.94	7.89	5.27	9.28	9.91	8.46	27.28	9.06	11.46	7.85	7.93	18.99
MgO	12.44	6.47	3.71	4.29	5.66	2.64	3.62	3.28	3.89	7.07	5.97	4.75	3.86	2.87
CaO	1.48	0.00	1.45	1.26	1.53	0.28	1.11	1.05	0.38	0.74	0.28	1.44	1.09	0.16
Na_2O	1.79	0.52	0.88	0.72	1.19	0.57	0.78	0.51	0.12	0.76	0.32	0.00	0.55	0.91
K_2O	0.86	1.00	2.19	0.64	1.19	2.73	2.01	2.52	7.38	6.45	7.23	7.77	9.11	7.47
TiO_2	1.63	3.60	1.99	0.74	0.49	0.76	0.97	1.07	0.37	0.67	1.28	0.78	1.01	0.77
IV Si	3.70	3.88	3.95	3.93	3.92	3.99	3.98	3.98	3.76	3.85	3.92	3.57	3.62	3.57
IV Al	0.30	0.12	0.05	0.07	0.08	0.01	0.02	0.02	0.24	0.15	0.08	0.43	0.38	0.43
VI Al	0.41	0.84	0.90	1.32	1.30	1.31	1.19	1.29	0.19	0.93	0.86	1.18	1.16	0.75
VI Fe^{3+}	0.72	0.74	0.72	0.35	0.24	0.43	0.46	0.39	1.39	0.44	0.56	0.38	0.39	0.95
VI Mg	1.20	0.62	0.35	0.38	0.50	0.24	0.34	0.29	0.39	0.67	0.58	0.45	0.38	0.28
Ca	0.11		0.10	0.08	0.10	0.02	0.07	0.07	0.03	0.05	0.02	0.10	0.07	0.01
Na	0.22	0.06	0.11	0.09	0.13	0.07	0.09	0.06	0.02	0.09	0.03	0.00	0.07	0.12
K	0.07	0.08	0.17	0.05	0.13	0.21	0.15	0.20	0.64	0.52	0.59	0.64	0.75	0.63
(060)	1.515	1.513	1.506	1.498	1.499	1.502	1.501	1.500	1.509				1.504/1.509	

— Large part of lithologic Unit 5
— Middle and upper Eocene and upper Oligocene

As above, quartz and feldspars are the most dominant non-clay minerals in the bulk sediment. Well-crystallized smectite is the most important clay mineral (70 to 100%, Plate 1-2); it is very aluminous and very often of beidellite type (d = 060–1,500 Å). Smectite is associated with chlorite (trace to 15%) and illite (5 to 20%); contrary to section 1, illite exhibits the classical morphology of a detrital illite (flakes with unprecise contours).

Mineralogical Unit 3

— Samples 104-643A-44X-3, 85–87 cm to -643A-14H-3, 87–89 cm
— 413.85 to 122.87 mbsf
— Dark mudstones and occurrence of silica
— Lithologic Unit 4 and most of lithologic Unit 3
— Lower Miocene and part of middle Miocene

This mineralogical unit may be subdivided into three subunits:

Mineralogical Subunit 3a

— Samples 104-643A-44X-3, 85–87 cm to 104-643A-33X-2, 91–93 cm
— 413.85 to 305.51 mbsf
— Mudstones
— Lithologic Unit 4
— Lower Miocene

The bulk sediment samples contain small quantities of quartz and feldspars (yet, feldspars are more abundant than quartz). Smectite in the clay fraction is abundant (60 to 100%) and always of dioctahedral nature. Illite amounts vary from 0 to 20%, chlorite and kaolinite are absent or occur in traces. The clay fraction contains amorphous silica and opal CT.

Electron microscopy (Plate 1-3) revealed the existence of numerous siliceous and dissolved biogenic debris, smectites with curled edges, and opal CT lepispheres (Samples 104-643A-44X-3, 85–87 cm; -643A-39X-2, 81–83 cm; -643A-38X-2, 94–96 cm; -643A-33X-2, 91–93 cm.

Although lithologic Unit 4 is composed of terrigenous mudstones (Eldholm, Thiede, Taylor, et al., 1987) typically detrital minerals are rare or absent (quartz, chlorite, kaolinite).

Mineralogical Subunit 3b

— Samples 104-643A-32X-2, 91–93 cm to -643A-29X-3, 64–66 cm
— 305.51 to 267.54 mbsf
— Mud and diatom ooze
— Top of lithologic Unit 4 and lowermost part of Unit 3
— Lower Miocene

This is a transitional subunit and although slightly different from the previous one, it has the peculiarity of containing, in the fine fraction, chlorite, kaolinite, quartz, and no opal CT.

Mineralogical Subunit 3c

— Samples 104-643A-28X-4, 130–132 cm to -643A-14H-3, 87–89 cm
— 259.90 to 122.87 mbsf
— Rich in biologic silica (diatom ooze)
— Most of lithologic Unit 3
— Lower Miocene and lowermost middle Miocene

Non-clay sediments of the total fraction contain few to no feldspars; quartz occurs in very small amounts except in Sample 104-643A-24X-3, 112–114 cm where it reaches 30%. Calcium carbonate content is observed toward the top of this subsection, and occurs in Sample 104-643A-16H-3, 90–92 cm.

In spite of an irregular evolution of the fine fraction, there is a sharp decrease in the smectite content with an associated increase of both chlorite, and to a lesser extent, kaolinite. The greater dispersal of d (060) values reveals the polygenic character of smectites which in the previous sections are not only better crystallized but also display a more homogenous chemical composition. Electron microscopy (Plate 1-4) shows siliceous biogenic debris that are less altered than in Subunit 3a, flack-shaped smectites, and fine interbedded laths corresponding to smectites growing within the sediment (Holtzapffel and Chamley, 1986).

Mineralogical Unit 4

— Samples 104-643A-13H-4, 114–116 cm to -643A-1H-2, 112–114 cm
— 115.44 to 2.62 mbsf
— Diatom nannofossil ooze to siliceous mud and mud
— Top of lithologic Unit 3 and lithologic Units 2 and 1
— Middle and upper Miocene, Pliocene, and Pleistocene

This mineralogical assemblage is characterized by the occurrence of quartz and mixed layer minerals in the fraction <2 μm. It may be divided in two mineralogical subunits:

Mineralogical Subunit 4a

— Samples 104-643A-13H-4, 114–116 cm to -643A-7H-4, 88–90 cm
— 115.44 to 58.18 mbsf

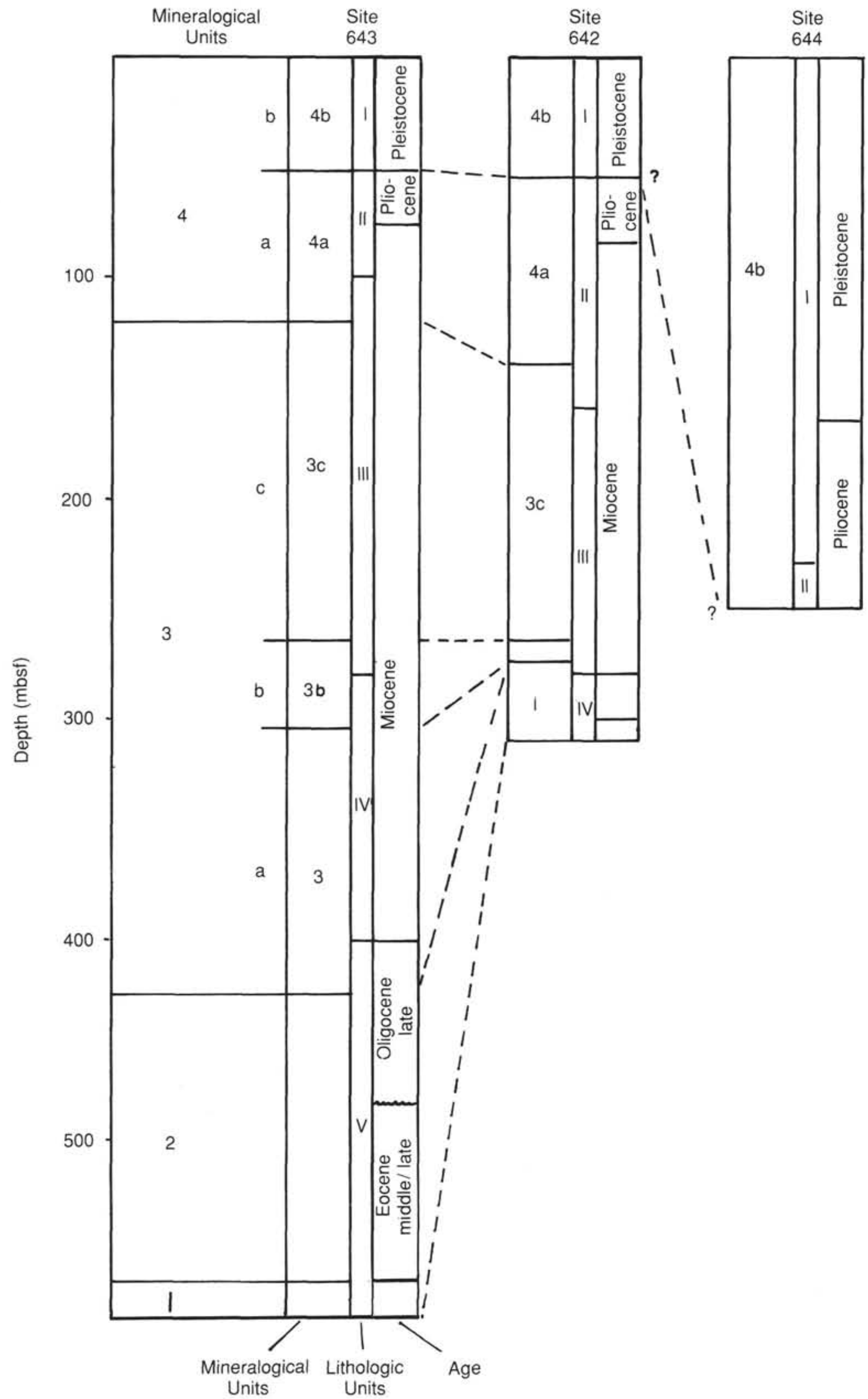

Figure 2. Mineralogical units and stratigraphy from Sites 642, 643, and 644.

Table 2. X-ray diffraction mineralogical results, Hole 643A.

		Bulk sediment•			Fraction <2 μm: Clay minerals★					Fraction <2 μm: Associated minerals				
Sample interval in cm	Depth (mbsf)	Calcite	Quartz	Feldspar	Chlorite	Illite	Inter-layer	Smectite	Kaolinite	Quartz	Feldspar	Amphi-bole	Amorphous silica	Opal CT
104-643A-1-2, 112–114	2.62	27	17	15	25	31	14	18	12	P	P			
2-2, 110–112	7.90	2	24	15	18	39		28	15	T	P			
3-3, 108–110	18.88	13	12	7	14	37		31	18	P				
4-4, 89–91	29.69		17	25	23	32	7	26	12	P	P			
5-6, 36–38	41.66		18	20	17	36	5	34	8	P	P			
6-3, 109–111	47.39		14	18	20	30	8	30	12	P	P			
7-4, 88–90	58.18	10	11	11	18	24	7	41	10	T			P	
8-4, 43–44	67.23		17	10	8	24	6	46	16	T	P		P	
9-5, 90–91	78.70	4	11	2	15	26	6	30	23	T	T		T	
10-4, 81–91	86.61	17	6	6	13	17	8	42	20	T	T		T	
12-4, 117–119	105.97		6		12	15	6	55	12	T	P		P	
13-4, 114–116	115.44		8		12	15	7	56	10	T			P	
14-3, 87–89	122.87		4		18	16		56	10	T			P	
15-3, 88–90	132.68		8		15	25		50	10	T			P	
16-3, 90–92	142.20	11	5		19	27		36	18				P	
18-2, 90–92	159.70		5	6	10	13		67	10				P	
20-3, 84–86	180.14		4		15	T		70	15				P	
22-4, 90–92	200.70		4		18	T		72	10				P	
23-4, 52–55	210.12		4		16	26		48	10				P	
24-3, 112–114	219.02		30	6	8	13		71	8				P	
25-4, 86–88	230.06		2		20	20		40	20				P	
26-3, 65–67	238.15		3		T	5		90	5				P	
27-5, 129–131	251.59		4		6	8		80	6				P	
28-4, 130–132	259.90		4		9	15		67	9				P	
29-3, 64–66	267.54		6	8				100		T			P	
31-4, 92–94	288.92		6	8	5	17		76	2	T				
32-2, 91–93	295.70		8	8	5	15		77	3	T			P	
33-2, 91–93	305.51		5	8	8	25		63	4	T			P	P
34-2, 15–17	315.31		8	8	T	11		89	T				P	P
35-1, 95–97	323.61		6	7	T	20		80	T				P	P
36-3, 90–92	336.40		5	8	T	14		86	T				P	P
37-4, 94–96	347.74		3	8				100					P	P
38-2, 94–96	354.54		4	7	T	18		82	T				P	P
39-2, 81–83	364.11		5	8	T	19		81	T				P	P
42-3, 98–100	394.68		5	8		17		83					P	T
44-3, 85–87	413.85		4	10		15		85						P
45-3, 88–90	423.58		10	9	7	16		77						
46-3, 90–92	433.30		12	6	9	15		76						
47-2, 66–68	441.26		6	8	8	18		74						
48-3, 60–62	452.30		9	8	9	18		73						
49-3, 67–69	462.07		6	8	11	12		77	T					
51-3, 99–101	481.69		18	9	7	12		81	T					
52-3, 106–108	491.36		9	8	5	8		87		P				T
53-6, 90–93	505.40		7	10	3	12		85						
54-2, 90–92	509.10		25	8				100		P				
55-5, 41–42	522.81		10	6	12	12		76		T	P			
57-4, 68–70	540.78		12	11	T	19		81		T				
60-2, 105–107	557.45		6	9	21	29		50	T	P			P	
61-1, 80–82	562.00			17				100						
62-1, 79–80	564.49		10	6	16	21		63		P				

• Total sample %; ★ in % with respect to all crystallized clay minerals studied; T: trace; P: present.

— Mud and diatom ooze (Plate 1-5)
— Upper part of lithologic Unit 3 and most of Unit 2
— Middle and upper Miocene and Pliocene

Quartz increases toward the top, in the bulk sediment fraction. Feldspars and calcite appear in Sample 104-643A-10H-4, 81–91 cm.

In the clay fraction, smectite is always abundant in spite of a decrease of 60% to 35%, while illite (20% to 30%), chlorite (10% to 20%) and kaolinite (10% to 30%) increase distinctly. Swelling mixed layer clay minerals occur from Samples 104-643A-13H-4, 114–116 cm upward. Quartz and feldspars appear in small amounts at the base of the subunit and increase to the top while amorphous silica remains constant. As in Subunit 3c, the mineralogy and crystallochemistry of smectites suggest varying origins.

Mineralogical Subunit 4b

— Samples 104-643A-6H-3, 109–111 cm to -643A-1H-2, 112–114 cm
— 47.39 to 2.62 mbsf
— Mud, sandy mud, and calcareous mud
— Upper part of lithologic Unit 2 and Unit 1
— Pleistocene

Quartz and feldspars are very abundant in the bulk sediment and percentages of calcite range from 0 to 20%.

The decrease of smectite described above (40–20%) in the clay fraction is well confirmed; in contrast, illite (25–40%) and chlorite (15–30%) increase notably; kaolinite percentages remain constant (10–20%). Mixed layer minerals are abundant. Quartz and feldspars occur always in abundant quantities in the fraction <2μm while amorphous silica disappears.

Site 642

Site 642 was drilled at five places, separated from each other by a distance of 450 m:

Hole 642E

A 914-m volcanic section was drilled from 315 to 1229 mbsf. This sequence has been divided into a lower and upper series separated by a 7-m thick volcaniclastic layer that corresponds to

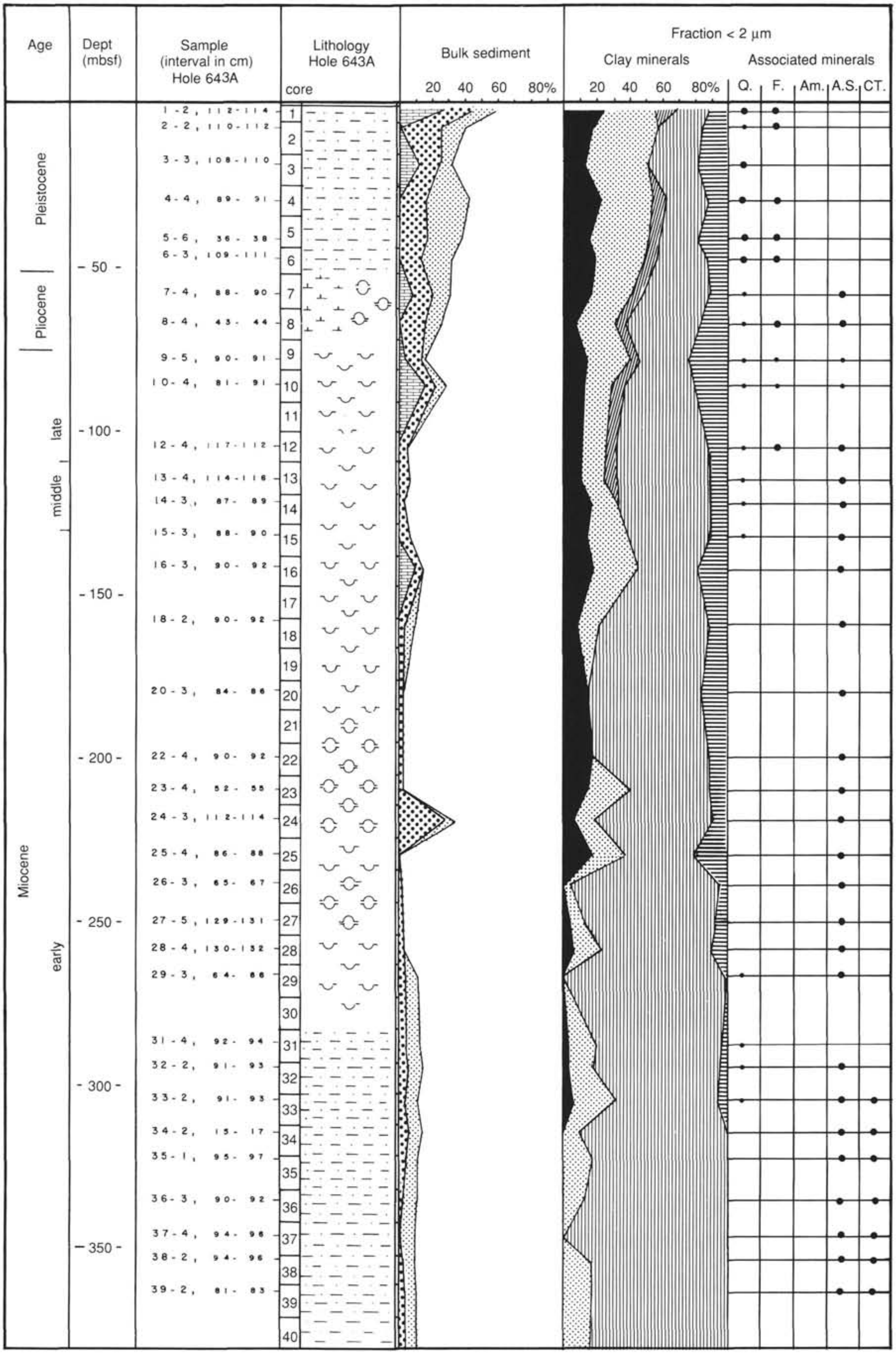

Figure 3. Mineralogical log, Hole 643A.

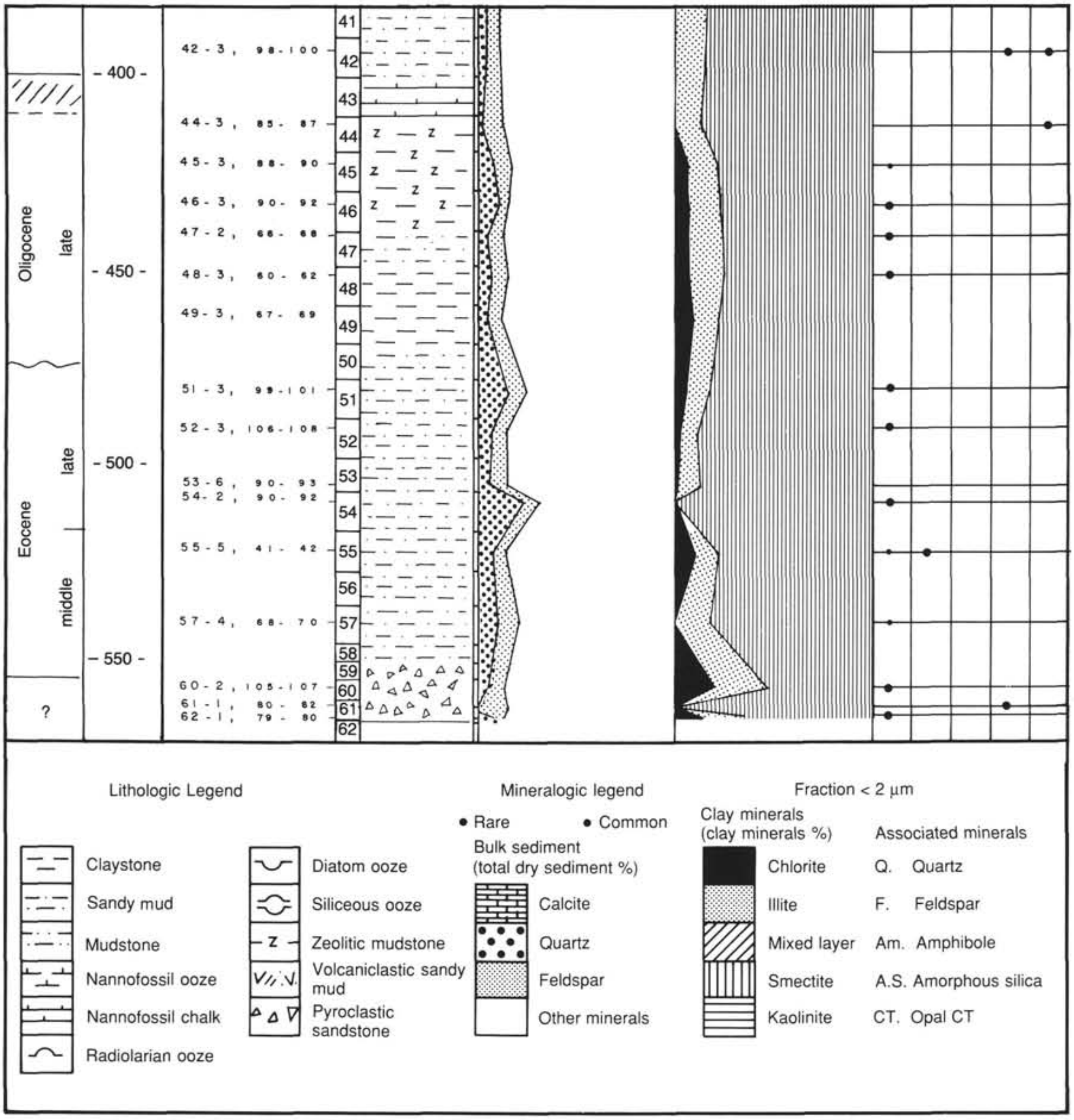

Figure 3 (continued).

reflector K on regional seismic profiles (Eldholm, Thiede, Taylor, et al., 1987); only this volcaniclastic layer is analyzed here.

The three samples analyzed (104-642E-94R-4, 49–51 cm; -642E-94R-4, 100–102 cm; and -642E-94R-5, 7–8 cm), display the same clay fraction mineralogical composition. Smectite is poorly crystallized and of dioctahedral character [d(060) = 1.500 Å], attaining concentrations of 50% of the clay fraction, while kaolinite is 40%. Accompanying abundant minerals are quartz and goethite.

Holes 642D, 642C, and 642B

Holes 642D (Table 3, Fig. 4), 642C (Table 4, Fig. 5), and 642B (Table 5, Fig. 6) may be divided into mineralogical units that are correlated with mineralogical units distinguished at Site 643.

— Samples 104-642D-13X-2, 54–57 cm to -642D-11X-1, 130–131 cm
— 298.24 to 278.10 mbsf
— Volcaniclastic sandy mud, glaucony rich pyroclastic sand, and sandy mud
— Lithologic Unit 4
— Upper Eocene and non-dated sediment

Feldspars are abundant in the bulk sediment while quartz is rare if not absent. The clay fraction is composed of smectite (60–90%), illite (10–40%), chlorite (0–10%), and kaolinite (0–10%). It also includes quartz, feldspars and phillipsite. Measurements of d (060) suggest the existence of three types of smectites: aluminous dioctahedral (d = 1.500 Å), ferriferous dioctahedral (d = 1.510 to 1.515 Å), and trioctahedral ferro-magnesian (d = 1.525 Å). The last two smectites are associated with weathering of pyroclastic material (Desprairies et al., this volume); ferriferous smectites occur only in a green facies of "glauconitic sands" which ends with a hard ground (Eldholm, Thiede, Taylor, et al., 1987). Some illites reveal a lath facies (TEM) (Plate 1-6) similar to that already observed in mineralogical Unit 1 of Site 643.

These deposits are very similar to those of mineralogical Unit 1 at Site 643.

— Samples 104-642D-10X-3, 66–69 cm and -642D-9X-3, 50–52 cm

Table 3. X-ray diffraction mineralogical results, Hole 642D.

Sample interval in cm	Depth (mbsf)	Bulk sediment* Calcite	Bulk sediment* Quartz	Bulk sediment* Feldspar	Fraction <2 μm: Clay minerals★ Chlorite	Illite	Inter-layer	Smectite	Kaolinite	Associated minerals Quartz	Feldspar	Amphi-bole	Amorphous silica	Opal CT
104-642D-2-3, 50–52	193.40		4	7	5	15	5	60	15	T	T		T	
3-3, 50–52	203.10		4	T	T	14	5	65	16	T	T		T	
4-3, 50–52	212.70		4	T	4	14	5	57	20				T	
5-3, 50–52	222.40		2	8	T	17	5	55	23				T	
6-3, 50–52	232.00		2	T	T	13	5	67	15				T	
7-3, 50–52	241.70		3		3	15	5	62	15	T			T	
8-3, 50–52	251.30		2	T	5	13	5	72	5	T	T		T	
9-3, 50–52	261.00		4	T	8	17		62	13	T			T	
10-3, 66–69	270.76		4	4	2	12		83	3					
11-1, 130–131	278.10					45		55						•
12-2, 31–34	288.31			20		30		70		T	T			
12-2, 123–127	289.23				12	29		47	12					
12-2, 136–140	289.36					40		60						
13-1, 105–108	297.25		3	24	8	28		56	8					
13-1, 120–123	297.40		6	22	4	11		81	4					
13-2, 54–57	298.24		4	15	2	7		89	2					

* Total sample %; ★ in % with respect to all crystallized clay minerals studied; T: trace; P: present; •phillipsite.

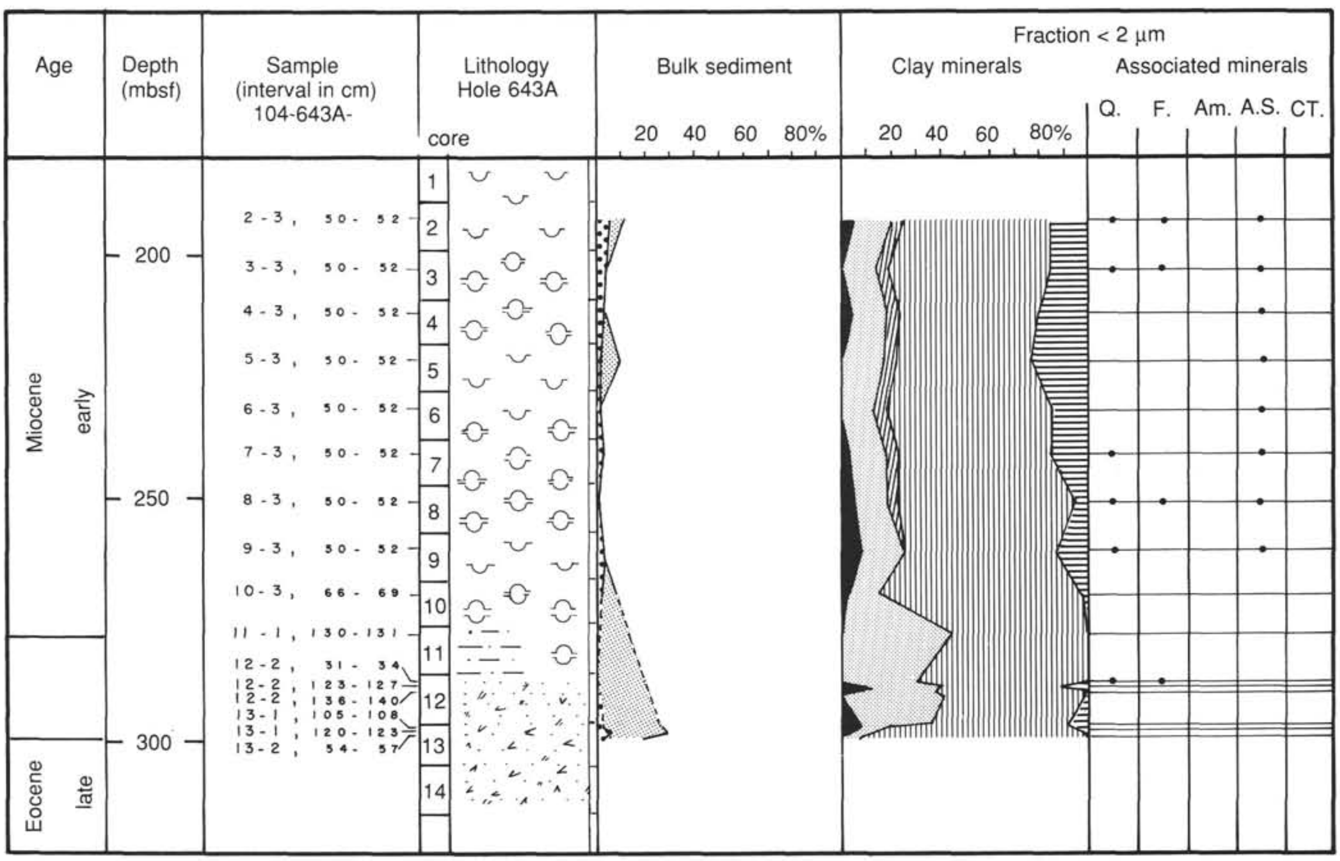

Figure 4. Mineralogical log, Hole 642D.

— 270.76 to 261.00 mbsf
— Muddy diatom ooze and muddy siliceous ooze
— Lower Miocene

These samples occur between two beds rich in glauconite and apatite (samples 104-642D-11X-1, 94–104 cm and -642D-8X-1, 85–120 cm, see Eldholm, Thiede, Taylor, et al., 1987). Quartz and feldspars are rare in the bulk sediment. The clay phase is chiefly composed of aluminous dioctahedral smectite (60–80%) associated with illite (15%), chlorite (5%) and kaolinite (10%). It also includes fine-grained quartz and amorphous silica.

This section may be compared to mineralogical Subunit 3b of Site 643. The mineralogical Subunit 3a of Site 643, characterized by opal CT at Site 643A, is absent here. This absence is emphasized by the occurrence of a hard ground observed in the middle of Core 104-642D-11X (Eldholm, Thiede, Taylor, et al., 1987).

— Samples 104-642D-8X-3, 50–52 cm to -642D-2X-3, 50–52 cm; 104-642C-24H-3, 85–87 cm to -642C-16H-3, 47–49 cm; and 104-642B-25H-3, 78–81 cm to -642B-14H-1 42–44 cm
— Hole 642D–251.30 to 193.40 mbsf

Table 4. X-ray diffraction mineralogical results, Hole 642C.

					Fraction $<2\ \mu m$									
		Bulk sediment*			Clay minerals★					Associated minerals				
Sample interval in cm	Depth (mbsf)	Calcite	Quartz	Feldspar	Chlorite	Illite	Inter-layer	Smectite	Kaolinite	Quartz	Feldspar	Amphi-bole	Amorphous silica	Opal CT
104-642C-2-3, 71-73	7.11	5	18	27	15	35	5	31	14	T	T			
4-3, 77-79	26.87	10	19	38	15	36	5	29	15	T	T	T		
5-3, 78-80	36.68	6	22	22	15	38	10	27	10	T	T	T		
6-3, 78-80	45.18		26	28	15	30	10	30	15	T				
7-3, 19-21	54.09		42	26	5	25	10	45	15	T	T	T		
8-3, 19-21	60.29		13	22	12	25	10	40	13	T	T			
10-3, 66-68	67.16	43	5	8	10	20	5	60	5	T	T	T	T	
11-3, 48-50	76.66	38	4	11	15	33	5	30	17			T	T	
12-3, 50-52	86.00		10	14	5	18	5	57	15				T	
13-3, 35-37	96.35		12	15	5	20	5	55	15	T		T	T	
14-3, 49-51	104.99	18	7	13	3	18	5	60	14	T	T		T	
15-3, 59-51	114.59		10	13	4	16	5	60	15	T	T		T	
16-3, 47-49	123.97		7	10	3	18	5	60	14				T	
17-3, 80-83	133.80	32	4		5	13	5	64	13				T	
19-3, 71-73	152.71		T	7	2	14	5	64	15				T	
19-3, 83-86	152.83	15	3	5	5	24	5	55	11				T	
20-3, 78-81	162.28		8	9	5	20	5	55	15				T	
21-3, 84-87	171.84		6	T	7	16	5	56	16				T	
22-3, 85-88	181.35		5	T	4	16	5	60	15				T	
23-3, 85-88	188.15		2	10	4	18	5	58	15				T	
24-3, 85-87	196.25		2	6	5	20	5	55	15	T	T		T	

* Total sample %; ★ in % with respect to all crystallized clay minerals studied; T: trace; P: present.

— Hole 642C–196.25 to 123.97 mbsf
— Hole 642B–216.88 to 114.42 mbsf
— Diatomaceous and siliceous mud and ooze
— Lithologic Unit 3, 2d and part of 2c

Chronostratigraphy

Bulk sediment includes small amounts of quartz (from a trace to 10%); feldspars are abundant especially at Hole 642B (from a trace to 25%). The first appearance of calcium carbonate level from the base of the hole occurs at the top of the mineralogical subunit (Samples 104-642C-19H-3, 83–86 cm and -642B-18H-3, 87–89 cm).

Within the fraction $<2\mu m$ the most dominant clay mineral is smectite whose chemical composition (060 values) is very variable (55–70%) followed by illite (15–20%), kaolinite (10–20%), mixed layer minerals (5–10%) and chlorite (0–10%). Associated minerals are quartz and feldspars that occur irregularly and in insignificant amounts; amorphous silica is present throughout the section.

The glauconite composition (Table 1, analysis 9) of the thin hard ground at the base of this mineralogical subunit (Sample 104-642D-8X-1, 85–120 cm, see Eldholm, Thiede, Taylor, et al., 1987), is very different from ferriferous illites (Table 1, analysis 10) analyzed at the base of Hole 643A.

These mineralogical and geochemical characteristics are similar to those of mineralogical Subunit 3c of Site 643.
— Sample 104-642C-15H-3, 59–51 cm to -642C-8H-3, 19–21 cm and Sample 104-642B-13H-3, 53–55 cm to 104-642B-9H-3, 60–62 cm
— Hole 642C–114.59 to 60.29 mbsf
— Hole 642B–107.73 to 70.00 mbsf
— Nannofossil ooze and mud
— Lithologic Unit 2 and part of lithologic Unit 1 for Hole 642C or lithologic Unit 2 for Hole 642B
— Upper Miocene and Pliocene

Within the bulk sediment, calcite exhibits two maxima which can be perfectly correlated between the two holes. Quartz and feldspars occur in the same proportions as in the previous episode.

Chlorite (5%) and illite (15–20%) within the fraction $<2\ \mu m$ occur in the same quantities as in lower sections almost throughout the subunit. Both minerals increase toward the upper part of the subunit, attaining 15 and 30% respectively. Smectite diminishes from 60% at the base of this episode to a maximum of 30% at the top. Kaolinite amounts vary slightly (15–20%). Associated minerals, e.g., quartz and feldspars, occur in fairly abundant quantities at the top of the interval. Amphiboles are found in the uppermost portions of this subunit and amorphous silica is present throughout the subunit.

These deposits have the same characteristics as those observed in mineralogical Subunit 4a of Site 643.
— Sample 104-642C-7H-3, 19–21 cm to -642C-2H-3, 71–73 cm
— Sample 104-642B-8H-3, 94–95 cm to -642B-1H-2, 67–69 cm
— Hole 642C–54.09 mbsf to the top
— Hole 642B–60.85 mbsf to the top
— Mud and foraminiferal mud
— Lithologic Unit 1
— Pleistocene

In bulk sediment, the calcite contents range from 0 to 10% in Hole 642C and 0 to 25% in Hole 642B. Quartz (10–25%) and feldspars (20-30%) increase sharply at the base of the section and remain abundant within the entire episode. Chlorite (10–15%) and illite (25–40%) are abundant in the clay fraction while smectite ranges from 30 to 50%. Mixed layer minerals vary between 5 and 10%, and kaolinite between 10 and 15%. Associated minerals consist of fairly abundant quartz, feldspars, and amphiboles, whereas opal disappears in the lower part of the episode.

These mineralogical assemblages correspond to mineralogical Subunit 4b of Site 643.

Site 644–Hole 644A (Table 6, Fig. 7) and Hole 644B (Table 7, Fig. 8)

Hole 644A

— Sections 104-644A-34H-3, 90 cm to -644A-1H-1, 63 cm
— 249.90 mbsf to the top
— Interbedded siliceous ooze and mixed siliceous nannofossil ooze at middle Pliocene
— Interbedded dark and light muds from upper Pliocene to Holocene

In the bulk sediment samples, calcite varies from 0 to 30%, quartz from 5 to 30% and feldspars from 5 to 30%. The latter

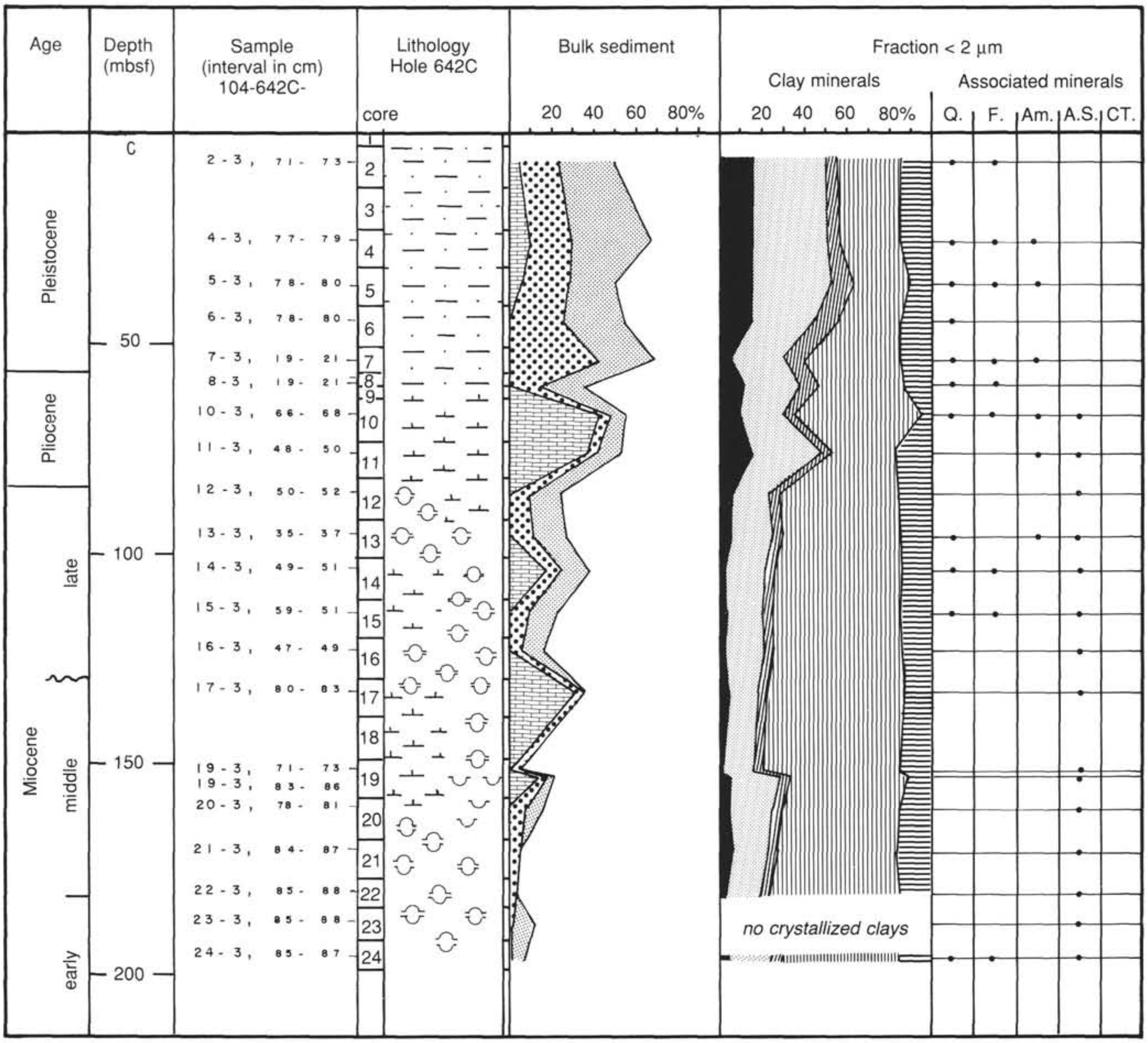

Figure 5. Mineralogical log, Hole 642C.

two minerals increase in abundance from the end of the Pliocene upwards (Core 104-644A-25H).

The most dominant minerals in the clay fraction are chlorite (5 to 35%) and illite (25 to 60%). Smectite percentages range between 5 and 50% while percentages of mixed layer minerals (0–15%) and kaolinite (5–30%) change very little.

Fluctuations in bulk and fine-fraction mineralogical assemblages are frequent and rapid. Mineralogical composition varies with the change of the color of the sediment: the black layers sampled (Samples 104-644A-14H- 3, 6–8 cm; -644A-13H-4, 137–139 cm; -644A-8H-3, 47–49 cm; -644A-6H-5, 92–96 cm; -644A-6H-3, 92–96 cm; and -644A-6H-1, 92–96 cm) show approximately the same mineralogical assemblages as those observed in the adjacent light layers. In the bulk sediment, smear slides show that calcite may be of biogenic or non-biogenic nature (Eldholm, Thiede, Taylor, et al., 1987). In fact, smectite maxima in the lower part of Hole 644A (Cores 104-644A-34H to -644A-15H) correspond to biogenic calcite maxima. Chlorite and illite maxima are associated with either lack of calcite (Cores 104-644A-29H to -644A-23H) or with nonbiogenic calcite maxima.

Hole 644A samples correspond to mineralogical Subunit 4b of Site 643.

Correlations can be made on the basis of comparative mineralogical data between the sites are shown in Figure 2. Boundaries between mineralogical units do not always correspond to boundaries between lithological units as observed elsewhere by Krissek (this volume).

Geochemical Composition of the Clay Fraction of Sediments

Chemical analysis of argillaceous-rich sediments selected in each mineralogical unit from Sites 642 and 643 was conducted on 41 samples. In some cases, i.e., Eocene and Oligocene sediments, clays are solely constituted of smectite and/or ferriferous-illite or glauconite. The composition of these samples as well as that of several samples from DSDP Leg 38 together with deduced structural formula are given in Table 1. The evolution

Table 5. X-ray diffraction mineralogical results, Hole 642B.

Sample interval in cm	Depth (mbsf)	Bulk sediment*			Fraction <2 μm: Clay minerals★					Fraction <2 μm: Associated minerals				
		Calcite	Quartz	Feldspar	Chlorite	Illite	Inter-layer	Smectite	Kaolinite	Quartz	Feldspar	Amphi-bole	Amorphous silica	Opal CT
104-642B-1-2, 67-69	2.14	12	16	27	15	28	5	37	15	T	T	T		
2-3, 50-52	8.30	25	12	21	10	30	10	40	10	T	T	T		
3-3, 84-86	18.14	12	22	32	13	30	5	37	15	T	T	T		
5-3, 56-58	32.96		26	32	10	25	5	50	10	T	T	T		
6-3, 70-72	42.60		26	31	10	20	5	55	10	T	T	T		
7-3, 92-94	51.32		16	31	13	35	10	32	10		T	T		
8-3, 95-97	60.85		26	30	10	31	10	41	8	T	T	T		
9-3, 60-62	70.00	50	2	5	5	24	10	48	13					
10-3, 80-82	79.70	38	5	T	5	15	5	65	10				T	
11-3, 78-80	89.18	16	8	15	3	15	5	62	15				T	
12-3, 77-79	98.67		12	18	5	14	5	61	15				T	
13-3, 53-55	107.73	23	6	10	5	15	5	60	15				T	
14-1, 42-44	114.42		4	12	5	24	5	51	15				T	
15-3, 48-50	126.98	15	8	9	5	20	5	55	15				T	
16-3, 60-62	131.70	6	12	8	5	21	5	51	18				T	
17-3, 54-56	141.54	8	6	T	5	15	5	63	12				T	
18-3, 87-89	151.67	5	9	10	5	25	5	50	15				T	
19-3, 85-87	161.55		8	10	5	20	5	52	18				T	
20-1, 85-87	168.25		8	9	7	20	5	48	20				T	
21-3, 53-55	180.63		6	25	6	17	5	55	17				T	
22-3, 77-80	190.47		6	T	5	20	5	52	18				T	
23-3, 78-80	199.78		8	10	T	25	5	50	20				T	
24-3, 78-81	209.38		5	T	8	25	5	52	10				T	
25-3, 78-81	216.88		4	T	5	21	5	54	15				T	

* Total sample %; ★ in % with respect to all crystallized clay minerals studied; T: trace; P: present.

of the chemical composition of phyllites may be traced with the help of constitutive element ratios. Al, instead of Si, is used as a reference element because of the frequent occurrence of silica in the <2-μm sediment fraction (Fig. 9).

In Table 1 and Figure 9, maximum values of 060 reflection—observed on X-ray powder diagrams of the same fraction—are given.

Smectites

- Lower (?) and middle Eocene. Weathered pyroclastic levels between Cores 104-643A-54X and -643A-62X are marked by the exclusive occurrence of ferromagnesian smectites of saponite type (Table 1, analysis 1). In the same interval, mudstones are characterized by the presence of dioctahedral smectites and highly variable illite and chlorite amounts. The same mineralogical association exists in Hole 642D, within an interval of undifferentiated Eocene age (Cores 104-642D-11X to -642D-14X). Within this latter section, muds are composed of dioctahedral smectites of beidellite type (Table 1, analyses 4–5) and volcaniclastic sands of trioctahedral smectites. This clear contrast in interbedded lithologies is observed in deposits of the same age from DSDP Leg 38, both in Cores 38-343-5 to -343-16, drilled in the same water depth as Site 643-and in Cores 38-338-30 to -338-42 close to Site 642. These DSDP Leg 38 deposits contain only ferromagnesian smectites (Table 1, analyses 2–3).
- Upper Eocene to upper Oligocene. The deposits of this period are absent or condensed at Site 642 but well developed at Site 643. Diatom muds of lithologic Subunits 2c and 2d at Site 338 (DSDP Leg 38) could correspond to these deposits. Smectites, still the most dominant minerals in the clay fraction, have a remarkably homogenous geochemical composition. Although dioctahedral and aluminous, they differ from the lower to middle Eocene smectites by their distinctly poor Mg contents (Table 1, analyses 6, 7, and 8). This difference is reflected in geochemical profiles (Fig. 9) by a sharp increase in the Al/Mg ratio; such an increase is not, however, associated with a sensitive change in the Al/Fe ratio.
- Lower Miocene. Because of the occurrence of primary minerals and silica in diatom muds in Hole 642D (Cores 104-642D-11X to -642D-6X) and in terrigenous muds in Hole 643A (Cores 104-643A-43X to -642-30X) the rigorous chemical composition of smectites cannot be clearly determined; smectites remain nevertheless the prevailing minerals of the clay fraction. As above, Mg and Fe geochemical profiles are opposed. This opposition implies that these elements are almost exclusively linked to the variability of the composition of smectites which are beidellite with various Fe contents.
- Lower Miocene to Holocene. The dominant characteristic in diatom and terrigenous muds at all sites is the concordance of Mg and Fe profiles. The chemical composition of smectites deposited during the Pliocene, Pleistocene and early Miocene, is aluminous, whereas during the late Miocene it became ferriferous. This period is also marked by a decrease in the Al/K ratio in contrast with underlying sediments.

Glauconites and Ferriferous-magnesian Illites

Glauconites

The Eocene to lower Miocene deposits at Site 642 display frequent occurrences of glauconite. This ferro-magnesian and potassic mineral is characterized by low Al contents (Table 1, analysis 9). In most cases, glauconite appears to be an *in-situ* weathering product of volcanic glass: several ash layers (Sections 104-643A-28X-1 and -642D-8X-1) show the entire transformation of this product from fresh glass-whether of an acid or basic composition-into glauconite (cf. Desprairies et al., this volume). Glauconite is often associated with apatite and is found in sedimentary formations where important gaps have been observed, especially throughout the middle Eocene and Oligocene at Site 642.

Ferriferous-magnesian Illites

These micaceous particles were described in mineralogical Unit 1 of Hole 643A. SEM and EDS analyses of these particles yielded a chemical composition (Table 1, analyses 10 and 11) quite different from that of glauconites because of their high contents of Al and from that of detrital illite-micas by high contents of Fe-Mg. Ferro-magnesian illite has also been observed in ash layers associated with glauconite (Desprairies et al., this vol-

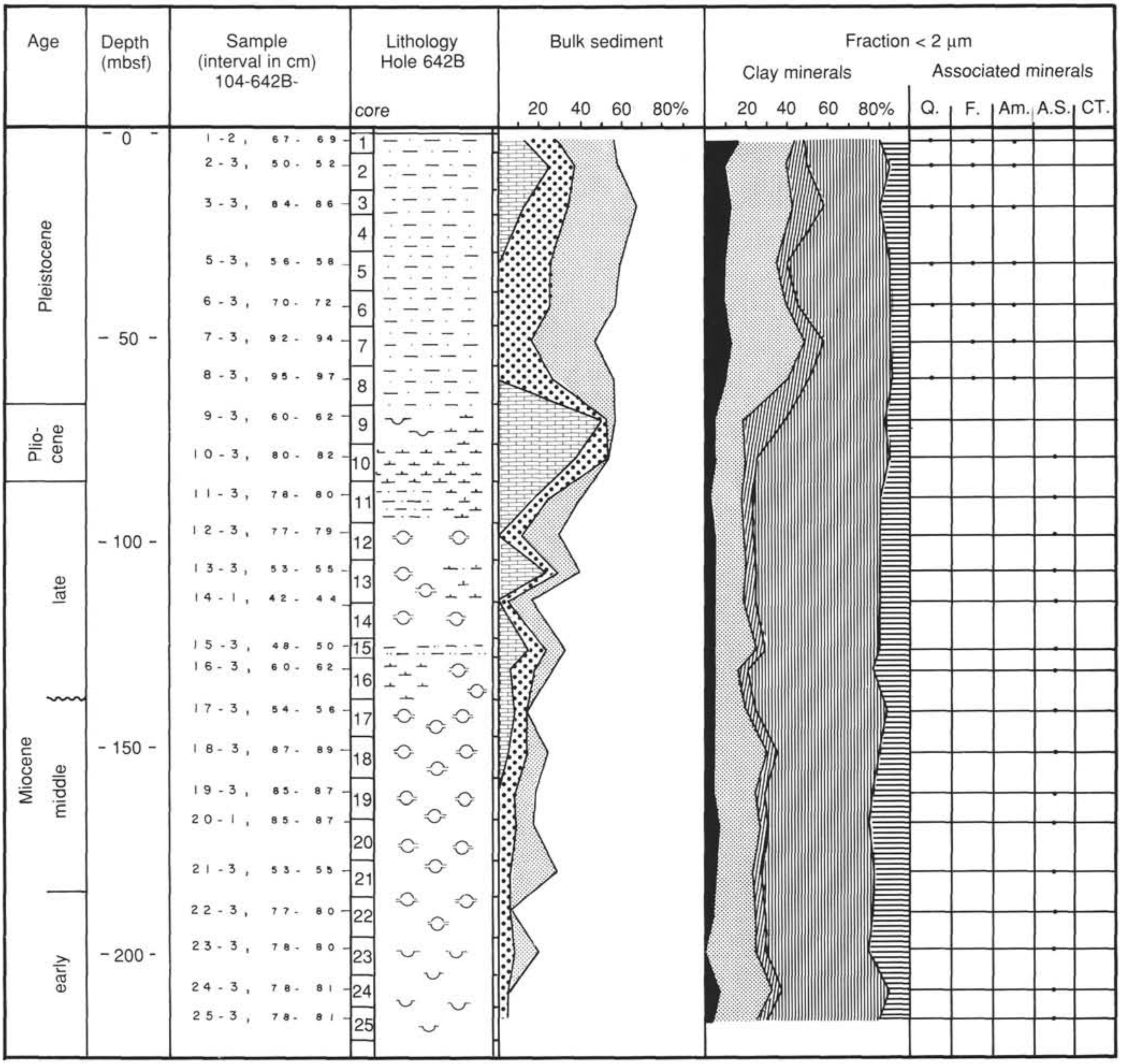

Figure 6. Mineralogical log, Hole 642B. (Key to symbols used is given in Fig. 3.)

ume) and in dissiminated particles within smectite-rich bed (Table 1, analyses 6, 7, 8). This mineral could have a specific significance for the clay fraction in Eocene and lower Miocene sediments.

DISCUSSION

The reconstruction of paleoenvironments on the basis of mineralogical and geochemical data requires a good knowledge of diagenetic changes and volcanic contribution. For this study all possible origins and the significance of minerals were considered in the light of several works.

In the case of Leg 104 sediments, some minerals have a particular significance. Examples are quartz, feldspars, amphiboles, illite, and chlorite which often occur in crystalline and metamorphic rocks. Their presence in marine sediments suggests the dismantling of these rocks, caused either by tectonic action or by mechanical erosion (Millot, 1964; Griffin et al., 1968; Chamley, 1971). Calcite is most often marine but may also originate from erosion of calcareous continental formations (Biscaye, 1965; Chamley, 1971). Opal CT is generally considered to be derived from early diagenesis of biogenic silica or to be eroded from exposed outcrops (Griffin et al., 1972).

The origin of smectite is variable. It may be of pedogenetic origin as kaolinite and part of irregular mixed layer minerals. Smectite may also occur during various stages of diagenesis. Finally, it may, more than any other mineral, result from weathering of volcanic material (Yeroschev-Shak, 1964; Bonatti, 1967; Paquet, 1969; Chamley, 1979).

Diagenetic Effects

Geochemical profiles of clay fractions at Sites 642 and 643 (Fig. 9) show a correlation between variations in the Al/Ti and Al/K ratios and between Al/Fe and Al/Mg ratios. Gieskes and Lawrence (1981) implied that the Al/Ti variation can be attributed to the presence of volcanic material. This suggestion cannot be retained here because the ash particles in Miocene to Pleistocene deposits are not, or are very poorly, altered into clays. The covariation between K and Ti and variations in the Al/K ratio are attributed to the presence of micas of detrital origin. Below the lower Miocene section the primary detrital phase composed of illite-micas and chlorite is scarce, whereas smectites are predominant. Within this same interval, ferriferous, ferro-magnesian illite becomes abundant and is associated with smectites of equally ferro-magnesian nature. A smaller Al/K ratio reveals, therefore, the progressive replacement of smectites by ferriferous illites during postburial diagenesis in the pre-Miocene section. Micaceous minerals are generally considered as a sink for pore-water K. In the case of ODP Leg 104, analysis of the K content in pore water was not done. Nevertheless, results obtained from all sites drilled during DSDP Leg 38, which are very close to the ODP Leg 104 sites, show a K depletion in pore water, attributed to the reaction of pore water with surrounded sediments (Gieskes et al., 1976). Another argument in favor of a diagenetic origin for ferro-ferriferous illites is the paleotemperature estimation from oxygen isotope analysis. Measurements of the illite fraction of Sample 104-643A-61X-1, 190 cm (Table 1, analysis 10) yielded a ^{18}O vs. Standard Mean Ocean Water (SMOW) at 18.5‰. Assuming that formation in equilibrium occurs with water at 0‰ and that when using the fractionation factor for glauconite (Savin and Epstein, 1970), a temperature of formation at 40° C is obtained, the hypothesis of a detrital origin for mica at this same temperature in this sample must be rejected.

Al/Mg and Al/Fe ratios are covariant from lower Miocene to Pleistocene; the opposite occurs below the lower Miocene. Analysis of pore waters shows an increase in Ca and a decrease in Mg towards the base of Sites 642–643. Similar trends observed by Gieskes and Lawrence (1981) in many DSDP sites could, according to these authors, indicate alteration of volcanic material both in the sedimentary column and/or at the basement. The same processes could have occurred at Site 642. Saponites derived from weathered Eocene pyroclastic elements could have trapped magnesium from pore water during a postdiagenetic process. Thus diagenetic effects concerning clay minerals appear below the lower Miocene while a "diagenetic front" also occurs below 250 mbsf. The physical proprieties of the sediment change rapidly, and more compact fabric and opal CT appear (Site 643) at these depths.

Volcanic Contribution to the Genesis of Clay Minerals

- Glauconites issued from *in-situ* weathered volcanic glass are the result of early diagenesis throughout an alteration stage at water-sediment interface and before burial (Odin, 1979).
- Ash layers from Pleistocene to lower Miocene are just slightly weathered. This interpretation is limited to the clay fraction associated with these layers. From a qualitative point of view, the composition of this clay fraction is identical to that of sediments bordering the ash layers; no preferential neogenesis of smectites indicating alteration of glass has been noted. Smectites appear therefore to be essentially detrital from the lower Miocene to Pleistocene. This is not, however, the case from upper Eocene to lower Miocene. Diagenesis is responsible for the *in-situ* alteration of pyroclastic elements into trioctahedral smectites of an increasingly ferro-ferriferous illite species.

PALEOENVIRONMENTAL RECONSTRUCTION

The Base of Cenozoic Sedimentation

The most clayey levels of reflector K (Eldholm, Thiede, Taylor, et al., 1987), found between the lower and upper series of lava flows, contain only dioctahedral and poorly crystallized smectite and kaolinite. Thus the kaolinite/smectite assemblage and the absence of primary clay minerals (illite and chlorite), despite the proximity of micaceous sandstones, suggest these sediments developed as continental soils under a hot and moist climate (Paquet, 1969). This interpretation agrees with that of Nilsen and Kerr (1978), who maintain that lateritic Paleocene soils existed in the Lofoten Basin. Identical assemblages have also been observed in lower Eocene Rockall sediments (DSDP Leg 81, Site 555, Latouche and Maillet, 1984) and Faeroe Iceland Ridge (Parra et al., 1986).

Eocene (Mineralogical Unit 1)

Sediments are marked by high smectite content. Their mineralogical characteristics suggest two possible origins of smectite sources. As indicated above, trioctahedral smectites (ferriferous saponites) originate in all likelihood from the *in-situ* alteration of pyroclastic material. Conversely, dioctahedral smectites (ferriferous beidellites), whether their parent rock is volcanogenic or not, derive from badly drained continental soils developing under a hot climate with contrasted seasonal humidity (Millot, 1964; Paquet, 1969).

Middle Eocene to Upper Oligocene Sediments (Mineralogical Unit 2)

Smectite is still the dominant mineral. It occurs in the form of a beidellite and, as in underlying units, indicates the persistence of continental soils under a hot climate with contrasting seasons. However, the occurrence of chlorite (sensitive to hydrolysis) and fine (<2 μm) quartz (whose size could probably be characteristic of eolian input) suggests a drier climate. Minerals, e.g. quartz, feldspars, illite, and chlorite thought to be derived from terrigenous inputs (Chamley, 1979), indicate erosion probably associated with tectonic action responsible for the opening of the Norwegian Sea during early Eocene (Roberts and Montadert, 1979). Eocene detrital inputs with the same mineralogical assemblages have been observed in far greater amounts at Sites 338 and 343 of DSDP Leg 38 (Froget 1981). The differences in Eocene detrital input between Legs 104 and 38 sites may be due either to the large contrasts in structural morphology of the Norwegian margin, or to diachronism of the deposits.

Lowermost Miocene (Mineralogical Subunit 3a)

Dioctahedral smectites continue to be the most abundant minerals and are thought to have derived from soils from a hot and moist climate; this assumption is supported by the disappearance of chlorite destroyed by hydrolysis (Loughnan, 1969).

The abundance of silica and the lack of fine detrital material in these sediments suggest the existence of a vegetation cover in the sediment source area that is sufficiently thick to trap particles and allow at the same time evacuation of solutions rich in silica. During this episode, diagenetic phenomena (solution, precipitation) must have changed the initial composition of sediments by provoking partial transformation of amorphous silica into opal CT (Williams et al., 1985; Williams and Crerar, 1985) and probably favoring further formation of smectites from this excess of silica (Chamley and Millot, 1972; Badaut and Risacher, 1983).

Diatoms in the lowermost Miocene section were detected on smear slides (Eldholm, Thiede, Taylor, et al., 1987) but very weathered debris were observed with the electron microscope. Most of the amorphous silica in these sediments probably originated from siliceous organisms (diatoms). The development of diatoms could have been accentuated by the presence of dissolved continentally-derived silica, or by coastal upwelling rich in nutritive elements.

Table 6. X-ray diffraction mineralogical results, Hole 644A.

					Fraction <2 μm									
		Bulk sediment•			Clay minerals★					Associated minerals				
Sample interval in cm	Depth (mbsf)	Calcite	Quartz	Feldspar	Chlorite	Illite	Inter-layer	Smectite	Kaolinite	Quartz	Feldspar	Amphi-bole	Amorphous silica	Opal CT
104-644A-1-1, 63	0.63	7	15	19	12	36		36	16					
1-5, 63	6.63	8	11	13	11	47	T	28	14			T		
2-1, 6	9.26		19	30	18	33	4	14	31			T		
2-3, 66	12.86	9	15	17	13	29	5	42	11			T		
2-3, 96–98	13.16	7	29	12	29	37	4	12	18	P	P			
2-5, 65	15.85	12	15	25	14	35	4	31	16	T				
3-1, 112	17.32	8	25	11	15	36		34	15					
3-3, 90–92	20.10	1	14	13	25	49	2	6	18	T	P			
3-5, 112	23.32	7	13	11	12	38	5	31	14		T	T		
4-1, 92	26.62	5	20	17	10	30	8	39	13		T			
4-3, 92	29.62	6	18	13	12	33	8	33	14		P			
4-5, 92	32.62	6	16	13	11	39	7	30	13	T	T			
5-3, 92	39.12	8	15	24	13	31	4	36	16			T		
5-4, 92–94	40.62	12	9	9	22	48	3	6	21	T	T			
5-5, 92	42.12	9	18	24	15	29	3	38	15		T	T		
6-1, 92	45.62		30	24	18	25	6	33	18		P			
6-3, 92	48.62	7	13	13	13	40	4	30	13		T			
6-5, 92	51.62	12	13	13	15	33	4	33	15		T	T		
8-1, 45	64.17	4	18	15	14	30	3	36	17		T	T		
8-3, 47	67.17	9	15	11	13	31	4	36	16	T	P	T		
8-5, 110–111	70.80		14	17	24	49	4	8	15	T	P			
9-1, 90	74.10	16	18	17	15	41		29	15		T			
9-3, 113–115	77.33	7	10	14	30	38	T	18	14	T	P			
9-5, 90	80.10	5	16	17	14	46	2	20	18		T	T		
10-1, 44	83.14	5	13	13	13	42	2	30	13	T	T			
10-3, 63–65	86.33	20	12	11	25	42	2	19	12	T	T			
10-5, 44	89.14	7	19	11	10	28	2	48	12	T	T			
11-1, 112	93.32	3	15	13	16	35	4	29	16		T	T		
11-3, 112	96.32	12	12	17	12	37	2	33	16		T			
11-5, 95–97	99.15		12	13	20	47	3	11	19	T	P			
12-1, 55	102.25		17	17	12	32	4	36	16					
12-4, 85–87	107.05	8	6	13	27	41	3	17	12	T	T			
12-6, 55	109.75		14	13	10	39	4	34	13	T	T	T		
13-1, 114	112.34	5	13	13	36	55	T	6	3	T	P			
13-4, 137–139	117.07		18	18	22	32	6	20	20	P				
14-2, 112	123.32	4	16	20	14	48	7	17	14	T	T	T		
14-3, 6–8	123.76	11	12	30	22	49	T	7	22	T	P			
14-4, 112	126.32	7	11	20	34	50	T	8	8	T	P	T		
15-1, 90	131.10		13	20	31	49	7	4	9	T	P	T		
15-3, 90	134.10		16	17	30	44		19	7	T	P	T		
15-5, 90	137.10	10	11	13	24	48	8	12	8	T	T	T		
16-1, 88	140.58	21	11	12	13	39	9	26	13		T			
16-2, 88–90	142.08		14	15	21	49	4	5	21	T	P			
16-5, 88	146.58		13	13	24	52	4	12	8	T	P	T		
17-1, 55	149.75		15	16	28	38	10	14	10	T	P	T		
17-2, 55–57	151.21	10	12	13	22	40	6	17	15	T	P			
17-5, 55	155.75		13	15	18	47	4	13	18	T				
18-1, 88	159.58		17	18	34	49	7	0	10	T	P	T		
18-2, 88–90	161.08		14	17	20	44	4	12	20	T	P			
18-5, 88	165.58	6	16	15	21	42	7	13	17	T	T	T		
19-3, 90	169.10	10	14	17	27	49	6	9	9	T	T	T		
19-4, 90–92	173.60		12	14	16	49	4	15	16	T				
20-1, 90	178.60	9	14	12	17	50	4	12	17	T		T		
20-2, 90–92	180.10	13	15	15	21	44	4	17	14	T				
20-5, 90	184.60	3	13	13	31	50	4	4	11		T			
21-1, 95	185.75	2	13	15	25	45	5	15	10	T	T	T		
21-2, 5–7	186.35		15	14	22	41	T	22	15	T				
22-2, 46–48	188.76		14	14	24	45	T	15	16	T				
22-3, 46	190.26	4	11	13	12	40	T	32	16	T	T			
22-5, 46	193.26		12	15	13	29	3	40	15	T		T		
23-2, 92	196.06		12	17	22	42	7	7	22	T		T		
23-3, 92–94	198.02		11	14	20	47	4	10	19	T	T			
23-4, 92	199.52		13	17	21	51	T	16	12	T	P	T		
24-1, 90	202.01		18	20	20	48	4	15	13	T	T	T		
24-2, 91–93	203.51		13	25	34	40	4	7	15	T	P			
24-3, 91	205.01		13	12	20	52	8	8	12		T			
25-1, 96	206,96		17	13	25	50	5	10	10	T	T	T		
25-2, 90–92	208.40		13	23	25	47	5	10	13	P				
26-1, 111	211.61		12	13	18	40	12	12	18					
26-2, 111–113	213.11		14	14	19	46	4	12	19	T	T			
27-1, 95–97	215.25		12	13	23	50	4	7	16	T	P			
28-1, 90	217.00		13	17	16	44	4	20	16					
28-2, 90–92	218.50		10	12	17	48	4	14	17	T	P			
28-3, 90	220.00		12	11	17	52	5	9	17					
29-1, 90	222.00		12	11	21	55	3	7	14	T	P	T		
29-2, 90–92	223.50		14	12	17	43	4	17	19	T				
29-3, 90	225.00		11	11	14	25	3	38	20	T		T		
30-1, 90	227.00		13	19	15	34	T	38	13	T	T			
30-2, 90–92	228.50	10	8	8	16	36	3	25	20	T	T			
30-3, 90	229.19		10	12	23	45	9	9	14					
31-1, 90	233.00		11	11	19	50	6	6	19	T				

• Total sample %; ★ in % with respect to all crystallized clay minerals studied; T: trace; P: present.

Table 6 (continued).

Sample interval in cm	Depth (mbsf)	Bulk sediment*			Fraction <2 µm: Clay minerals*					Associated minerals				
		Calcite	Quartz	Feldspar	Chlorite	Illite	Inter-layer	Smectite	Kaolinite	Quartz	Feldspar	Amphi-bole	Amorphous silica	Opal CT
31-2, 90-91	234.50		11	11	17	45	6	15	17					
31-3, 90	236.00		12	20	28	48	4	8	12			T		
32-1, 90	239.00	2	13	20	13	43	13	18	13					
32-2, 90-92	240.50	17	11	9	15	28	6	34	17	P				
32-3, 90	242.00	14	11	15	17	44	11	11	17			T		
33-1, 90	244.46	16	9	6	20	50	10	10	10		T	T		
33-2, 30-32	245.50	31	5	9	15	28	6	34	17	P				
34-1, 90	246.90		13	10	16	49	11	8	16		T			
34-2, 90-92	248.40		11	12	4	62	8	18	8	T				
34-3, 90	249.90	2	12	11	21	47	6	13	13		T			

Middle Lower Miocene (Mineralogical Subunit 3b)

Mineralogical characteristics are similar to those of mineralogical Subunit 3a, with the exceptions that there is less quartz and feldspar in the coarse fraction and chlorite and kaolinite occur in the clay fraction. This transitional episode reflects a warm temperate climate such as that in mineralogical Subunit 3a; however, the presence of limited amounts of chlorite indicates fewer hydrolysis effects.

Uppermost Lower Miocene to Middle Miocene Sediments (Mineralogical Subunit 3c)

Smectite is poorly crystallized and of a variable chemical composition; it decreases while primary minerals increase, especially chlorite. Trends observed in the previous episode are accentuated here especially with the establishment of a distinctly warm and dry temperate climate. However, the limited quantities of quartz and feldspars in the coarse and fine fractions imply that continental erosion was not intense.

At the top of this subunit, calcium carbonates appear for the first time while sediments remain essentially siliceous. The development of carbonate organisms cannot be solely due to warming of waters; it must have been also induced by a change in the oceanic circulation. At that time, the Iceland—Faeroe Ridge sill subsided (Berggren and Hollister 1974; Roberts and Montadert 1979; Berggren and Schnitker 1983) allowing water mass exchange between the Atlantic and the Norwegian Sea. Correlatively, the flow of Norwegian Sea water masses to the south is reflected in the early appearance of illites and chlorites (Latouche and Maillet, 1979, 1984) in sediments of the Rockall region (DSDP Legs 48B and 81).

Calcium carbonate in Holes 642B and 642C occurs a bit later than at Site 643. Site 642 was covered by Atlantic waters at a later date, given its proximity to the continent. It was also located in shallower depths than Site 643. A similar time lag exists, for identical reasons, between deposits of illites and chlorites at different Rockall sites.

Upper Miocene to Pleistocene Sediments (Mineralogical Unit 4)

Inherited clay minerals, quartz, feldspars, and amphiboles, increase considerably in the Pliocene toward the top of mineralogical Subunit 4a. Mixed-layer minerals were probably derived from continental weathering of crystalline and crystallophyllian rocks, linked to the recurrence of Scandinavian shield erosion due to climatic conditions. These detrital inputs, characterizing mostly the Pleistocene, are the direct result of the glaciation on the Scandinavian peninsula. This detrital material may have been transported in two ways: part of it was probably transported by floating ice (Talwani, Udintsev, et al., 1976) and the other part was probably derived from erosion of coastal moraines (Emelyanov et al., 1978).

The polygenic nature of smectites in this interval is an indication of their variable origin sources. Given their characteristics, smectites must have been formed in continental soils. The smectites may have been derived from the Scandinavian shield and/or reworked, as kaolinite (Krissek, this volume), from older sedimentary rocks from the Atlantic. If so, they must have been transported by S-N currents or even from soils on volcanic rocks (Iceland/Faeroes, Moyes et al., 1974).

A detailed study of Pliocene and Pleistocene sedimentary episodes has been made for Site 644. The dominant characteristic is the large variability of the smectite-illite-chlorite assemblage with kaolinite amounts remaining almost constant. These variations appear to be the result of climatic changes: smectite maxima could be associated with warm interglacial climates and illite and chlorite with glacial periods. Several arguments support this assumption: (a) smectite formation in continental soils requires moist and warm climatic conditions to allow for an efficient hydrolysis of rock minerals; (b) in the lower portion of Hole 644A (Cores 104-644A-34H to -644A-15H), smectite maxima correspond to biological calcite maxima (Cores 104-644A-34H to -15H). Marine microfaunas show that sediments were deposited during interglacial temperate climatic periods (Eldholm, Thiede, Taylor, et al., 1987). Cores 104-644A-34H to -644A-31H are marked by abundant diatoms and silicoflagellates as well as by the appearance of planktonic foraminifers indicating the existence of warm water masses. The same situation occurs between 180 and 200 mbsf (Cores 104-644A-23 to -644A-21) where once again smectite maxima occur; (c) the most recent sediments (Core 104-644A-1H) of interglacial facies correspond to smectite maxima; and (d) conversely, at 236 mbsf diatom studies (Eldholm, Thiede, Taylor, et al., 1987) indicate major cooling of surficial waters corresponding to chlorite and illite maxima.

Assuming that these correlations between mineralogy and climatic events apply to the entire sedimentary column, a paleoclimatic curve (Fig. 7) may be established for Pliocene-Quaternary deposits at Hole 644A by comparison of illite and chlorite vs. smectite.

ACKNOWLEDGMENTS

We are grateful to M. Chamley and C. Beck for their critical comments on this paper. Special thanks are extended to the ODP staff representative Elliott Taylor for his help and advice. This study was supported by ASP.-ODP.France.

REFERENCES

Badaut, D., and Risacher, F., 1983. Authigenic smectite on diatom frustules in Bolivian saline lakes. *Geochim. Cosmochim. Acta*, 47:363–375.

Berggren, W. A., and Hollister, C. D., 1974. Paleogeography, paleobiogeography and the history of circulation in the Atlantic Ocean. *Studies in Paleoceanography*, Soc. Econ. Paleontol. Mineral. *Spec. Publ.*, 20: 126–186.
Berggren, W. A., and Schnitker, D., 1983. Cenozoic marine environments in the North Atlantic and Norwegian Greenland Sea. *In* Bott, Saxov, Talwani, and Thiede (Eds.), *Structure and development of the Greenland-Scotland Ridge*: New York (Plenum), 495–548.
Biscaye, P. E., 1965. Mineralogy and sedimentation of recent deep sea clay in the Atlantic Ocean and adjacent seas and oceans. *Geol. Soc. Am. Bull.*, 76: 803–832.
Bonatti, E., 1967. Mechanisms of deep sea volcanism in the South Pacific. *Res. Geochem.* 2: 453–491.
Brindley, G. W., and Brown, G., 1980. *Crystal structures of clay minerals and their X-ray identification*: London (Mineralogical Society).
Brown, G., 1961. *The X-ray Identification and Crystal Structures of Clay Minerals*: London (Mineralogical Society).
Chamley, H., 1971. Recherches sur la sédimentation argileuse en Méditerranée. *Mem. Serv. Cart. Géol. Alsace-Lorraine*, 35.
_______, 1979. North Atlantic clay sedimentation and paleoenvironment since the late Jurassic. *In* Talwani, M., Hay, W., and Ryan, W.B.F., (Eds.), *Deep Drilling Results in the Atlantic Ocean. Continental Margins and Paleoenvironment, Proceedings:* Washington (Am. Geophys. Union), 342–361.
Chamley, H., Debrabant, P., Foulon, J., Girould d'Argoud, C., Latouche, C., Maillet, N., Maillot, H., and Sommer, F., 1979. Mineralogy and geochemistry of Cretaceous and Cenozoic Atlantic sediments off the Iberian Peninsula (Site 398, DSDP Leg 47B). *In* Sibuet, J. C., Ryan, W.B.F., et al., *Init. Repts. DSDP*, 47, Pt. 2: Washington (U.S. Govt. Printing Office) 429–449.
Chamley, H., and Millot, G., 1972. Néoformation de montmorillonites à partir de diatomées et de cendres dans les sédiments marins de Santorin (Méditerranée Orientale). *C. R. Acad. Sc. Paris*, 274: 1132–1134.
Chamley, H., and Robert, C., 1979. Late Cretaceous to Early Paleogene environmental evolution expressed by the Atlantic clay sedimentation. *In* Christensen, W. K., and Birkelund, E. (Eds.), *Cretaceous/Tertiary Boundary Events Symposium*, 2: Copenhagen (Univ. of Copenhagen), 71–77.
Chennaux, G., Esquevin, J., Jourdan, A., Latouche, C., and Maillet, N., 1984. X-ray mineralogy and mineral gecchemistry of Cenozoic Strata (Leg 80) and petrographic study of associated pebbles. *In* de Graciansky, P. C., Poag, C. W., et al., *Init. Repts., DSDP*, 80: Washington (U.S. Govt. Printing Office), 1019–1046.
Desprairies, A., 1983. Relation entre le paramétre b des smectites et leur contenu en fer et magnésium. Application à l'étude des sédiments. *Clay Minerals*, 18:165–175.
Eldholm, O., Thiede, J., Taylor, E., et al., 1987. *Proc., ODP, Init. Repts.*, 104: College Station, TX (Ocean Drilling Program).
Emelyanov, E. M., Blazchishin, A. I., Kharin, G. S., Lozovaya, N. G., and Zangalis, K. P., 1978. Mineral and chemical composition of sediments of the Vøring Plateau, DSDP Leg 38. *In* Talwani, M., Udintsev, G., et al., *Init. Repts. DSDP, Suppl.*, 38, 39, 40, 41: Washington (U.S. Govt. Printing Office), 31–44.
Froget, C., 1981. La sédimentation argileuse depuis l'Eocéne sur le plateau Vøring et à son voisinage, d'aprés le Leg 38 D.S.D.P. (Mer de Norvége). *Sedimentology*, 28:793–804.
Gard, J. A., 1971. *The electron-optical investigation of clays*: London (Mineralogical Society).
Gieskes, J. M., 1976. Interstitial water studies, Leg 38. *In* Talwani, M., Udintsev, G., et al., *Init. Repts. DSDP, Suppl.*, 38, 39, 40, 41: Washington (U.S. Govt. Printing Office), 121–133.
Gieskes, J. M., and Lawrence, J. R., 1981. Alteration of volcanic matter in deep sea sediments: evidence from the chemical composition of interstitial waters from deep sea drilling cores. *Geochimica et Cosmochimica Acta*, 45: 1687–1703.
Griffin, J. J., Windom, H., and Goldberg, E. D., 1968. The distribution of clay minerals in the world ocean. *Deep Sea Res.*, 15:433–459.
Griffin, J. J., Koide, M., Hohndorf, A., Hawkins, J. W., and Goldberg, E. D., 1972. Sediments of the Lau Basin rapidly accumulating volcanic deposits. *Deep Sea Res.*, 19, 139–148.
Holtzapffel, T., 1985. Les minéraux argileux, préparations, analyses diffractométriques et détermination. *Soc. Géol. du Nord.*, 12.
Holtzapffel, T., and Chamley, H., 1986. Les smectites latées du domaine Atlantique depuis le Jurassique supérieur: gisement et signification. *Clay Minerals*, 21:133–148.
Joint Committee on Powder Diffraction Standards, 1974. *Selected Powder Diffraction Data for Minerals*, first Ed., Pennsylvania, U.S.A.
Jones, J. B., and Segnit, E. R., 1971. The nature of opal. 1. nomenclature and constituant phases. *J. Geol. Soc. Aust.*, 18:57–68.
Loughnan, F. C., 1969. *Chemical weathering of the silicate minerals*: New York (American Elsevier).
Latouche, C., and Maillet, N., 1979. X-ray mineralogy studies. Leg 48, Rockall Region (Sites 403, 404, 405, and 406). *In* Montadert, L., Roberts, D. G., et al., *Initial Repts. DSDP*, 48: Washington (U.S. Government Printing Office), 665–676.
_______, 1984. X-ray mineralogy study of Tertiary deposits, Leg 81, Sites 552–555. *In* Roberts, D. G., Schnitker, D., et al., *Init. Repts. DSDP*, 81: Washington (U.S. Govt. Printing Office), 669–682.
Mélières, F., 1977. X-ray mineralogy studies, Leg 41, Deep Sea Drilling Project, eastern North Atlantic Ocean. *In* Lancelot, Y., Seibold, E. et al., *Init. Repts. DSDP*, 41: Washington (U.S. Govt. Printing Office), 1065–1086.
Millot, G., 1964. *Geologie des Argiles*: Paris (Masson et Cie).
Moyes, J., Duplessy, J. C., Gonthier, E., Latouche, C., Maillet, N., Parra, M., and Pujol, C., 1974. Les sédiments profonds actuels et pleistocènes récents de l'Atlantique nord-oriental et du sud de la mer de Norvège. *Coll. Int. Expl. Oceans, Bordeaux*, 4:1–15.
Nilsen, F. H., and Kerr, D. R., 1978. Turbidites, redbeds, sedimentary structures and trace fossils observed in DSDP leg 38 cores and the sedimentary history of the Norwegian Greenland Sea. *In* Talwani, M., and Udintsev, G., *Init. Repts. DSDP, Suppl.* 38, 39, 40, 41: Washington (U.S. Govt. Printing Office), 259–288.
Odin, G. S., 1979. Remarks concerning glauconitic materials collected during Leg 48. *In* Montadert, L., Roberts, D. G., et al., *Init. Repts. DSDP*, 48: Washington (U.S. Govt. Printing Office), 787–789.
Paquet, H., 1969. Evolution géochimique des minéraux argileux dans les altérations et les sols des climats méditerranéens et tropicaux à saisons contrastés, *Mém. Serv. Carte géol., Alsace-Lorraine*, 30.
Parra, M., Puechmaille, C., Dumon, J. C., Delmont, P., and Ferragne, A., 1986. Geochemistry of Tertiary alterite clay phases on the Iceland-Faeroe Ridge (northeast Atlantic), Leg 38, Site 336. *Chem. Geol.*, 54:165–176.
Robert, C., 1982. Modalité de la sédimentation argileuse en relation avec l'Histoire Géologique de l'Atlantique Sud [Thése Doct. és-Sc.], u Aix-Marseille II.
Roberts, D. G., and Montadert, L., 1979. Margin paleoenvironments of the northeast Atlantic. *In* Montadert, L., Roberts, D. G., et al., *Init. Repts. DSDP*, 48: Washington (U.S. Govt. Printing Office), 1143–1153.
Savin, S. M., and Epstein, S., 1970. The oxygen and hydrogen isotope geochemistry of clay minerals. *Geochimica et Cosmochimica Acta*, 34:25–42.
Talwani, M., Udintsev, G., et al., 1976. *Init. Repts. DSDP*, 38: Washington (U.S. Govt. Printing Office).
Thorez, J., 1975. *Phyllosilicates and Clay Minerals. A Laboratory Handbook for their X-ray analysis*: Dison, Belgique (Lelotte).
Weaver, C, E., and Pollard, L. D., 1973. *The chemistry of clay minerals. In* Devel. Sedimentology, 15: Amsterdam (Elsevier).
Williams, L. A., and Crerar, D. A., 1985. Silica diagenesis, II. general mechanisms. *J. Sediment Petrol.*, 55:312–321.
Williams, L. A., Parks, G. A., and Crerar, D. A., 1985. Silica diagenesis, I. Solubility controls. *J. Sed. Petrol.*, 55:301–311.
Yeroschev-Shak, V. A., 1954. Clay minerals of the Atlantic Ocean. *Sov. Oceanogr.*, 30-2:90–106.

Date of initial receipt: 23 March 1987
Date of acceptance: 7 January 1988
Ms 104B-112

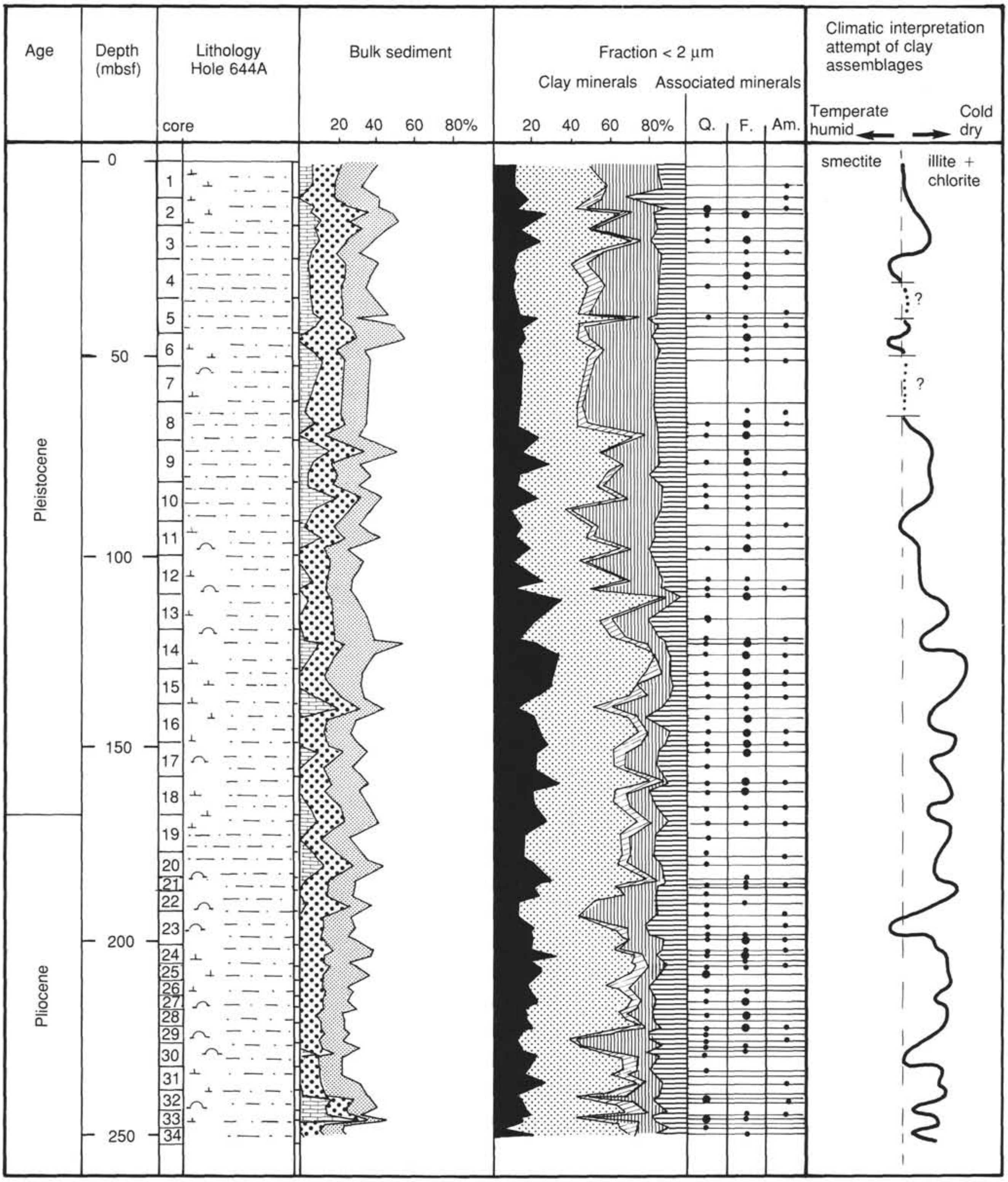

Figure 7. Mineralogical log, Hole 644A.

Table 7. X-ray diffraction mineralogical results, Hole 644B.

					Fraction <2 μm									
		Bulk sediment•			Clay minerals★					Associated minerals				
Sample interval in cm	Depth (mbsf)	Calcite	Quartz	Feldspar	Chlorite	Illite	Inter-layer	Smectite	Kaolinite	Quartz	Feldspar	Amphi-bole	Amorphous silica	Opal CT
104-644B-1-2, 70–71	2.20	8	21	15	25	46	T	9	20	T	P			
2-3, 70–71	8.30	12	11	14	31	54	T	8	7	T	P			
3-3, 70–71	17.80	10	16	14	23	47	T	7	23	P	P			
4-3, 70–71	27.30	7	12	15	23	44	3	9	21	P	P			
5-2, 33–34	34.93	7	13	14	25	42	T	14	19	T	P			
5-3, 33–34	36.43		18	28	23	33	6	20	18	P	P			
6-2, 56–57	44.66	15	11	14	22	48	T	8	22	T	P			
6-3, 56–57	46.16		31	30	19	68	T	5	8	T	P			
7-1, 47–48	52.57		40	35	30	32	4	22	12	T	P			
7-2, 47–48	54.07	4	15	10	20	42	6	20	12	T	T			
8-1, 68–69	62.28	10	18	14	19	27	4	22	28	T	P			
8-4, 88–89	66.98		30	17	17	30	5	18	30	T	P			
9-1, 66–67	71.76	2	28	18	33	40	T	10	17	P	P			
9-4, 134–137	76.94	7	14	15	30	54	T	T	16	T	P			
10-1, 105–106	81.65		19	35	26	42	3	8	21	T	P			
10-4, 109–110	86.19	18	12	14	20	37	7	23	13	T	P			
11-2, 63–64	92.23	17	13	12	23	27	6	12	32	P	P			
11-2, 102–103	92.62		18	19	20	47	4	9	20	T	P			
12-1, 70–71	96.60		17	26	28	38	4	17	13	T	P			
13-2, 14–15	106.34		21	27	20	33	4	14	29	T	P			
13-5. 6–7	109.76		15	34	20	47	4	9	20	T	P			
14-2, 30–31	115.96		12	14	25	48	T	6	21	T				
14-5, 123–124	118.63		20	28	28	35	T	20	17	T	P			
15-2, 70–71	121.4		11	14	21	40	4	14	21	T	P			

• Total sample %; ★ in % with respect to all crystallized clay minerals studied; T: trace; P: present.

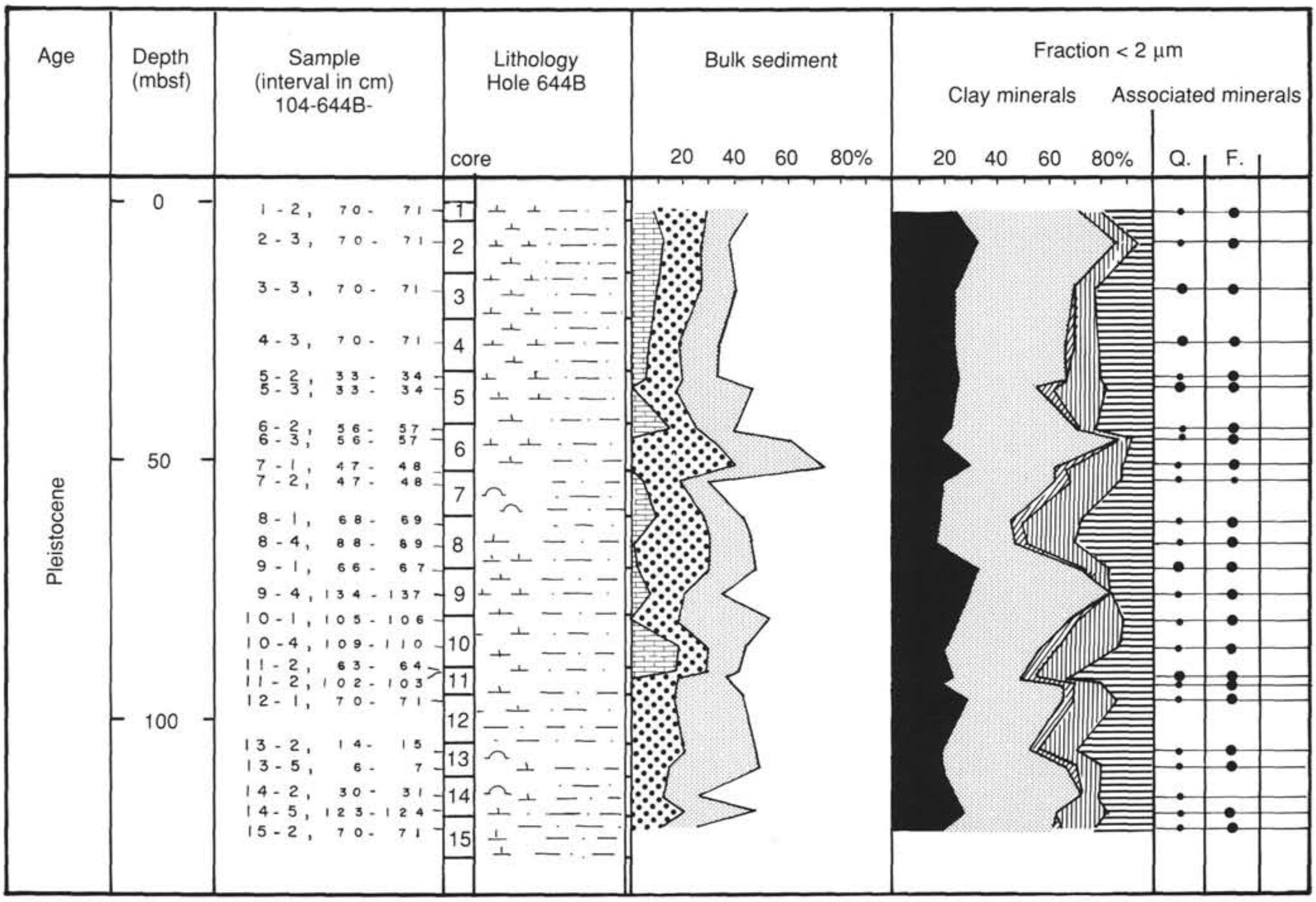

Figure 8. Mineralogical log, Hole 644B.

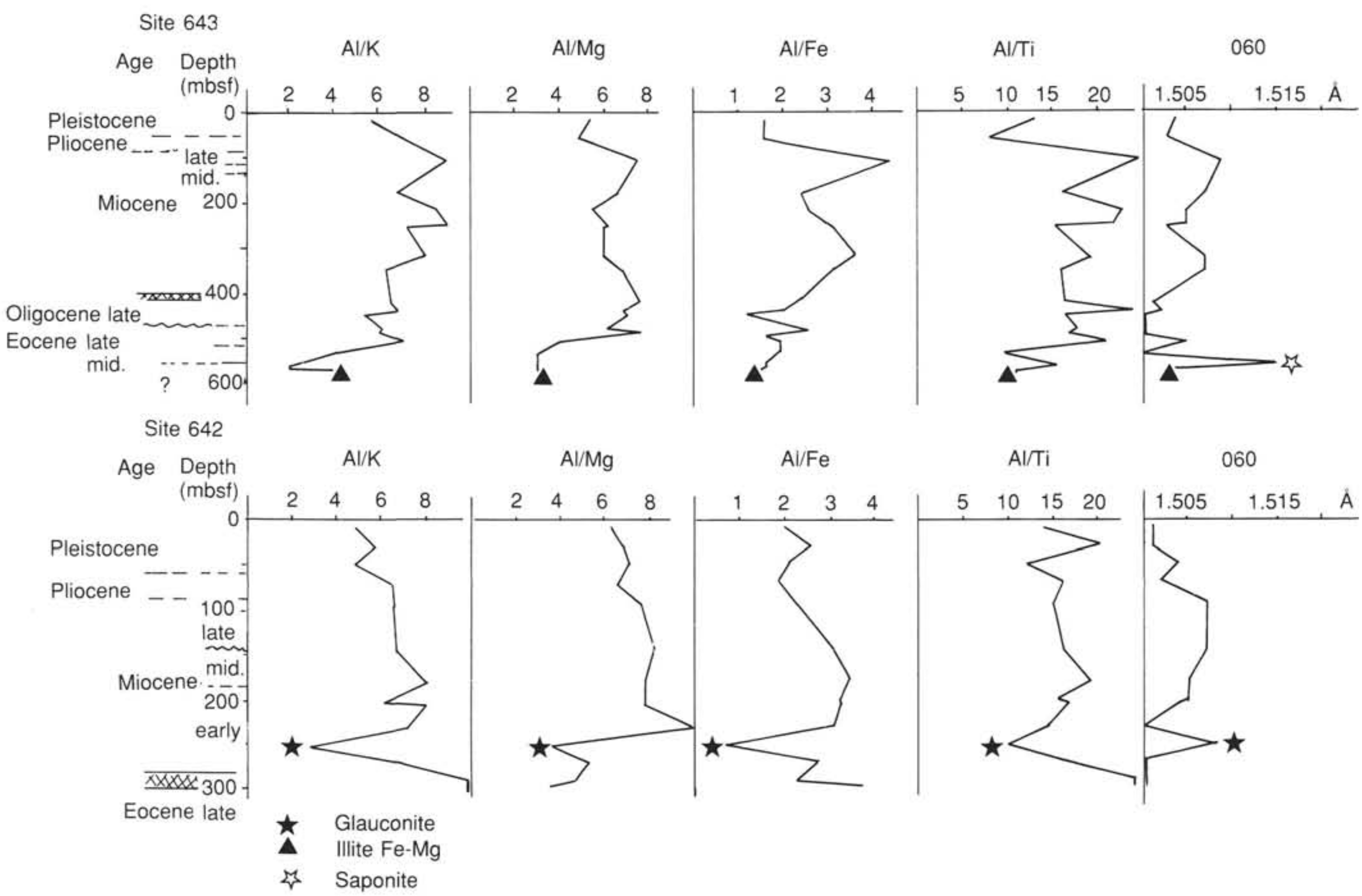

Figure 9. Elemental ratios of aluminium profiles for the clay fractions from Leg 104 sediments and 060 reflection.

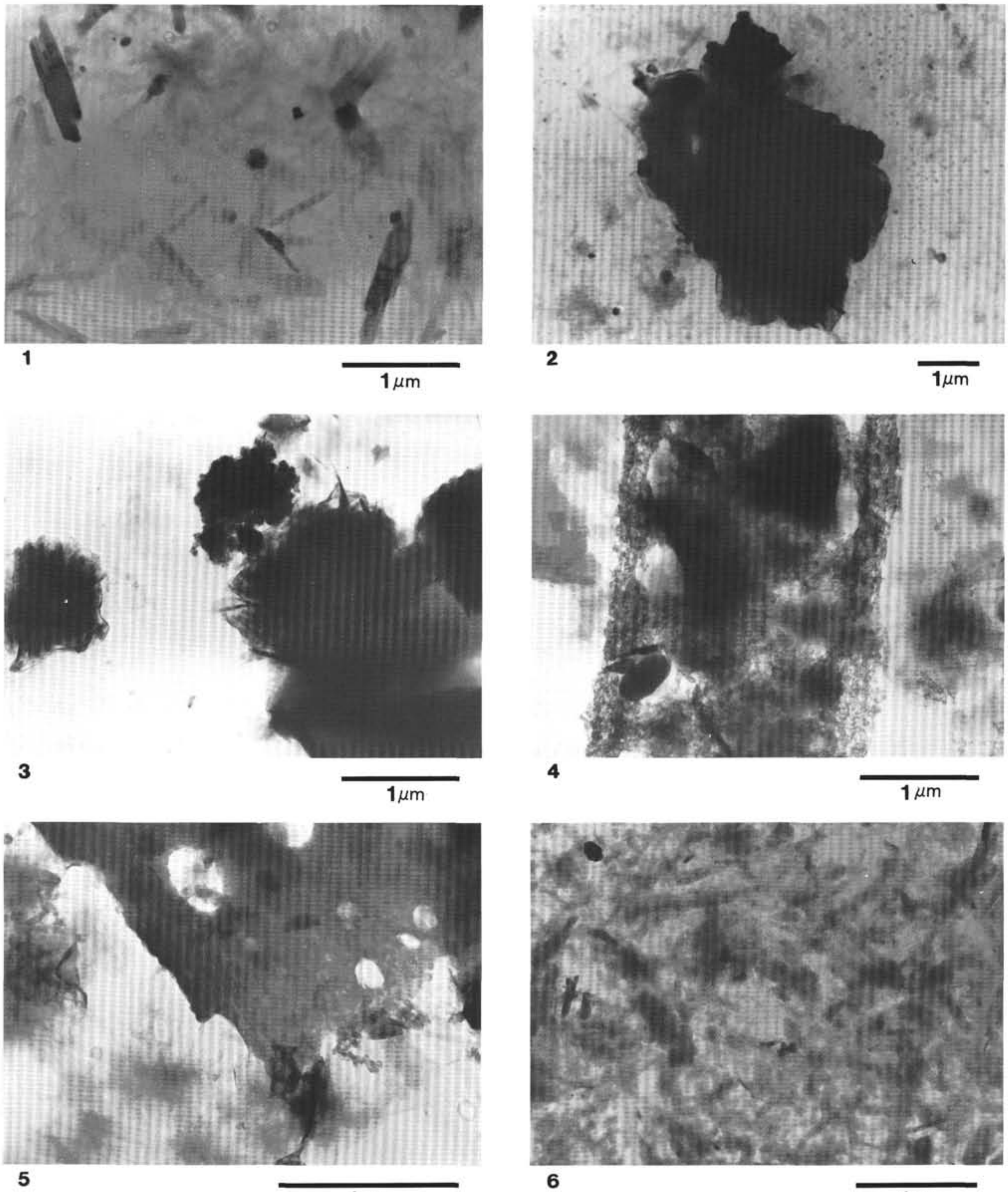

Plate 1. Leg 104 core samples. **1.** 10-Å clay mineral (ferriferous magnesian illite species). Sample 104-643A-62X-1, 79–80 cm, mineralogical Unit 1 (non dated). Pyroclastic mudstones. **2.** Dioctaedral smectite (Beidellite type). Sample 104-643A-55X-4, 41–42 cm, mineralogical Unit 1, middle Eocene. Terrigenous mudstones. **3.** Biogenic siliceous debris, smectites with curled edges, and opal CT lepispheres. Sample 104-643A-33X-2, 91–93 cm, mineralogical Subunit 3a, early Miocene. Mudstones. **4.** Well-dissolved siliceous biogenic debris, flack-shaped smectites, and fine interbedded laths. Sample 104-643A-24X-3, 112–114 cm, mineralogical Subunit 3c, early Miocene. Diatom oozes. **5.** Siliceous biogenic debris, smectites, and fine interbedded laths. Sample 104-643A-8H-4, 43–44 cm, mineralogical Subunit 4a, Pliocene. Diatom nannofossil oozes. **6.** Lath facies illite (ferriferous—magnesian illite species). Sample 104-642D-12X-2, 136–140 cm, mineralogical Unit 1 (non dated). Volcaniclastic sandy muds.